Journal of Marine Science and Application (2024) 23: 844-866
https://doi.org/10.1007/s11804-024-00407-4

RESEARCH ARTICLE

Wave Attenuation due to Stratified Porous Structure with Stepped Seabed

Ashna Varghese[1], K.R. Athul Krishna[1] and D. Karmakar[1]

Received: 12 July 2023 / Accepted: 18 February 2024

Abstract

The wave interaction with stratified porous structure combined with a surface-piercing porous block in a stepped seabed is analysed based on the small amplitude wave theory. The study is performed to analyse the effectiveness of partial porous structure in increasing the wave attenuation in the nearshore regions consisting of stratified porous structures of different configurations using the eigenfunction expansion method and orthogonal mode-coupling relation. The hydrodynamic characteristics such as wave reflection coefficient, transmission coefficient, dissipation coefficient, wave force impact and surface elevation are investigated due to the presence of both horizontally and vertically stratified porous structures. The effect of varying porosity, structural width, angle of incidence, wavelength and length between the porous block and stratified structure is examined. The numerical results are validated with the results available in the literature. The present study illustrates that the presence of the stratified structure decreases wave transmission and efficient wave attenuation can also be easily achieved. The wave force acting on stratified structure can be decreased if the structure is combined with wider surface-piercing porous blocks. Further, the presence of stratified porous structure combined with porous block helps in creating a tranquil zone in the leeside of the structure. The combination of vertical and horizontal stratified porous structure with surface-piercing porous block is intended to be an effective solution for the protection of coastal facilities.

Keywords Stratified porous structure; Surface-piercing; Porous block; Stepped seabed; Eigenfunction expansion method; Wave force

1 Introduction

Coastal erosion is a threat to coastal community that can cause various risks, including property damage, loss of land and ecosystem. The construction and use coastal protection structures is necessary to protect coastline and coastal facilities from severe wave action. In order to dissipate the incoming wave energy and thereby aid in the creation of a calm and secure harbourage, porous structures are frequently used in coastal engineering. Several researchers have extensively studied the dissipation of incoming wave energy due to the presence of single-layer porous structure with uniform porosity and friction factor (Sollitt and Cross, 1972; Madsen, 1983; Darymple et al., 1991; Mallayachari and Sundar, 1994; Das and Bora, 2014; Sulisz, 1985) and vertical porous membrane (Koley and Sahoo, 2017; Ashok and Manam, 2022). Experimental studies are also conducted to study the hydrodynamic characteristics of porous structures (Kondo and Toma, 1972; Sollitt and Cross, 1972; Twu and Lin, 1990; Somervell et al., 2017). The design and construction of a stratified structure is found to be an effective solution for dissipating the maximum wave energy and creating a tranquillity zone. In addition, studies are being conducted for the development of new configurations of porous structures in order to achieve maximum wave energy dissipation.

Significant studies have been carried out on the dissipation characteristics of wave interaction with stratified porous structures. Yu and Chwang (1994) examined the wave motion through a porous structure consisting of two layers and noted that a limiting thickness exists for the structure, beyond which hydrodynamic coefficients remain constant with any further increase in thickness. Later, Twu and Chieu (2000) designed an offshore breakwater having min-

Article Highlights

- The hydrodynamic performance of stratified porous structure combined with a surface-piercing porous block in a stepped seabed is analysed using small amplitude wave theory.
- The effect of structural and geometrical parameters due to stepped bottom configuration are analysed for the compsite breakwater system.
- The wave attenuation charecteristics along with wave force experience on the stratified breakwater and porous block due to stepped sea-bed is analysed.

✉ D. Karmakar
dkarmakar@nitk.edu.in

[1] Department of Water Resources and Ocean Engineering, National Institute of Technology Karnataka, Surathkal, Mangalore-575025, India

imal wave reflection and transmission using complex eigenfunction method. The numerical and experimental study revealed that a multi-layer breakwater can reduce both wave reflection and transmission at a narrower width compared to a single-layer porous structure. Thereafter, Twu et al. (2002) studied the wave-damping characteristics of a vertically stratified porous breakwater under oblique wave action. Further, Liu et al. (2007) proposed a two-layer horizontally stratified rock-filled core for a perforated breakwater and studied the effect of perforated breakwater on wave reflection and wave force impact on the structure. Recently, Venkateswarlu et al. (2020a) studied the oblique wave transformation due to fully-extended two-layered, three-layered and two-layered submerged horizontally stratified structures using the eigenfunction expansion approach. The study concluded that the increase in porosity of surface layer and moderate friction factor enhances energy damping. The multiple structures are found to be useful if the structure width is high and for a fixed structural width, separating into several structures helps in achieving high wave damping.

Additionally, it is critical to comprehend and understand the effect of seabed topography on the hydrodynamic behaviour of coastal protection structures, as reported by various researchers in the literature. Das and Bora (2014) investigated the wave reflection by a vertical porous structure placed on a stepped seabed as two separate cases with two and multiple steps. The study reported that lower values of friction factor led to oscillation in the reflection coefficient which vanished for higher values of friction factor but for relatively long waves, the values of the angle of incidence did not affect the reflection coefficient whereas short waves resulted in lower reflection coefficient. Afterwards, Hu et al. (2019) conducted an analytical study for oblique scattering of monochromatic small amplitude wave trains by a stationary rigid multi-layered structure of rectangular cross-section for a combined floating and bottom-mounted permeable breakwater. Venkateswarlu and Karmakar (2020b) investigated the significance of seabed characteristics in wave transformation in the presence of a vertically stratified porous structure. The study noted that the wave energy dissipation increases with the increase in porosity of the seaward porous layer. The theoretical results are compared with Twu and Chieu (2000) and found to be in good agreement with the experimental observations. The study suggested that, for better wave blocking, porosity of the leeside porous layer can be kept minimal. The performance in wave reflection of the porous structure placed on a stepped seabed is found better compared to that on a uniform and elevated seabed whereas the structure placed on an elevated seabed showed a significant role in wave blocking. Tabssum et al. (2020) analysed wave interaction with a thick, porous breakwater in a two-layer fluid, which is particularly applicable to continental shelves, having bottom undulation. Later, Venkateswarlu and Karmakar (2020c) examined the wave interaction with multiple porous structures upon elevated seabed in the presence and absence of a leeward wall.

Several researchers performed studies on partial structures which can be combined with primary structures to understand the improvement of wave dissipation properties of composite structures. These partial structures are especially beneficial as they are economic, uses less construction material and has least environmental concerns. Sahoo et al. (2000) investigated the wave interaction with vertical permeable barriers of various configurations including surface-piercing, bottom-touching and fully submerged barrier using eigenfunction expansion and least-squares method. The study concluded that the presence of porous barrier helps in attaining a minimum value of reflection coefficient for a particular value of the porous-effect parameter. Liu and Li (2013) presented a new analytical solution for hydrodynamic coefficients of a surface-piercing porous breakwater. Karmakar and Guedes Soares (2014) investigated the interaction of surface gravity waves with multiple bottom-standing flexible porous barriers. The study suggested that these structures are effective in wave attenuation. Later, Koley et al. (2015) studied wave scattering by a surface-piercing and bottom-standing structure placed at a distance from a rigid wall. Further, Behera and Ghosh (2019) dealt with a surface-piercing flexible porous barrier near a rigid wall in the presence of step-type bottoms and concluded that using suitable combination of wave and structural parameters, this structure can be used as an effective breakwater.

On investigating the studies performed by previous researchers, it is noted that the combination of stratified porous structure with partial porous structure in the presence of elevated step is limited. So, in the present study, wave interaction due to the presence of horizontal and vertical stratified porous structure combined with surface-piercing porous block in stepped sea bottom is examined to understand the effect of the combined stratified structure with surface-piercing porous block on wave attenuation. Numerical modelling is carried out using the eigenfunction expansion method along with orthogonal mode-coupling relations. The numerical study on the horizontally and vertically stratified porous structure combined with the porous block is performed and further analysis is performed for the effect of varying porosity, structural width, angle of incidence and length between the porous block and stratified structure. The study performed on the wave interaction with stratified porous structure with stepped bottom is noted to attenuate the wave height in transited region and helps in the dissipation of incoming wave in the large extent. The presence of the stratified structure is observed to largely dissipate the wave energy as compared to single porous structure and the wave trapping phenomenon is also noted due to the stepped bottom resulting in attenuation of wave

height. The present study will be very helpful in the wave force reduction on the offshore facility and also useful in the dissipation of wave energy to create the tranquil region.

2 Mathematical formulation for stratified structure with porous block

The present study investigates the oblique wave interaction with stratified porous structure combined with a surface-piercing porous block placed on stepped sea bottom using the small amplitude wave theory. The porous structure is considered to have different layers of porosity in horizontal and vertical directions considering the wave direction. The structure with layers of different porosity is termed as stratified structure. The study is performed on both horizontally and vertically stratified porous structures consisting of two layers of different porosities and friction factors. The surface-piercing porous block is on the seaward side of the stratified porous structure. The horizontally stratified porous structure is placed over the first rigid step whereas the vertically stratified structure is over first and second rigid steps such that each layer is over each step. The thickness of both the porous layers are kept equal throughout the study. The physical problem is analysed in the two-dimensional cartesian coordinate system with x and z-axis in horizontal directions and the y-axis is considered positive downward. The structure is infinitely extended along z-direction with the wave considered to be obliquely propagating in x-direction with an angle θ.

The seabed is assumed to be impervious such that no flow is possible in a perpendicular direction. The porous structure is assumed to be fully-extended and the height is considered equal to the free surface. The fluid domain is divided into nine regions. In the case of horizontally stratified porous structure (Figure 1), the regions considered include the upstream open sea region $I_1^h \equiv (0 \leqslant x \leqslant \infty, 0 \leqslant y \leqslant h)$, porous block region $I_2^h \equiv (-a_1 \leqslant x \leqslant 0, 0 \leqslant y \leqslant a)$, region below porous block $I_3^h \equiv (-a_1 \leqslant x \leqslant 0, a \leqslant y \leqslant h)$, region between porous block and stratified porous block $I_4^h \equiv (-a_2 \leqslant x \leqslant -a_1, 0 \leqslant y \leqslant h)$, stratified structure region $I_5^h \equiv (-a_3 \leqslant x \leqslant -a_2, 0 \leqslant y \leqslant b)$, bottom stratified structure region $I_6^h \equiv (-a_3 \leqslant x \leqslant -a_2, b \leqslant y \leqslant h)$, open sea region above second rigid step $I_7^h \equiv (-a_4 \leqslant x \leqslant -a_3, 0 \leqslant y \leqslant h_3)$, open sea region above the third rigid step $I_8^h \equiv (-a_5 \leqslant x \leqslant -a_4, 0 \leqslant y \leqslant h_4)$ and downstream open region $I_9^h \equiv (-\infty \leqslant x \leqslant -a_5, 0 \leqslant y \leqslant h_5)$. In the case of vertically stratified porous structure (Figure 2), the regions include the upstream open sea region $I_1^v \equiv (0 \leqslant x \leqslant \infty, 0 \leqslant y \leqslant h)$, porous block region $I_2^v \equiv (-a_1 \leqslant x \leqslant 0, 0 \leqslant y \leqslant a)$, region below porous block $I_3^v \equiv (-a_1 \leqslant x \leqslant 0, a \leqslant y \leqslant h)$, open sea region between porous block and stratified porous block $I_4^v \equiv (-a_2 \leqslant x \leqslant -a_1, 0 \leqslant y \leqslant h)$, seaward porous layer over first rigid step $I_5^v \equiv (-a_3 \leqslant x \leqslant -a_2, 0 \leqslant y \leqslant h_2)$, leeward porous layer over second rigid step $I_6^v \equiv (-a_4 \leqslant x \leqslant -a_3, 0 \leqslant y \leqslant h_3)$, open sea region above third rigid step $I_7^v \equiv (-a_5 \leqslant x \leqslant -a_4, 0 \leqslant y \leqslant h_4)$, open sea region above the fourth rigid step $I_8^v \equiv (-a_6 \leqslant x \leqslant -a_5, 0 \leqslant y \leqslant h_5)$ and the downward open sea region $I_9^v \equiv (-\infty \leqslant x \leqslant -a_6, 0 \leqslant y \leqslant h_6)$.

It is assumed that fluid is inviscid, incompressible, irrotational and time harmonic with angular frequency ω. The velocity potentials in the respective regions are represented in the form $\phi_j(x, y, z, t) = \mathrm{Re}\left[\phi_j(x, y)\mathrm{e}^{\mathrm{i}(lz - \omega t)}\right]$, where $l = \gamma_{10} \sin\theta$ and γ_{10} is the progressive wave number in open water region. The velocity potentials in the respective regions satisfy the Helmholtz equation given by

$$\frac{\partial^2 \phi_j}{\partial x^2} + \frac{\partial^2 \phi_j}{\partial y^2} - l^2 \phi_j = 0, \text{ for } -\infty < x < \infty, 0 < y < h \quad (1)$$

The linearized free surface boundary condition for the open water and porous structure region is of the form

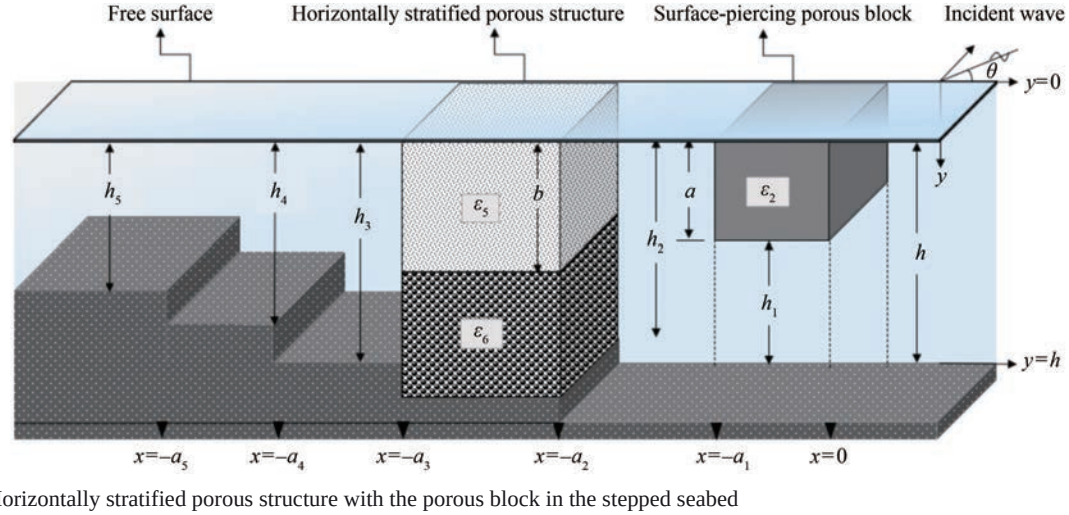

Figure 1 Horizontally stratified porous structure with the porous block in the stepped seabed

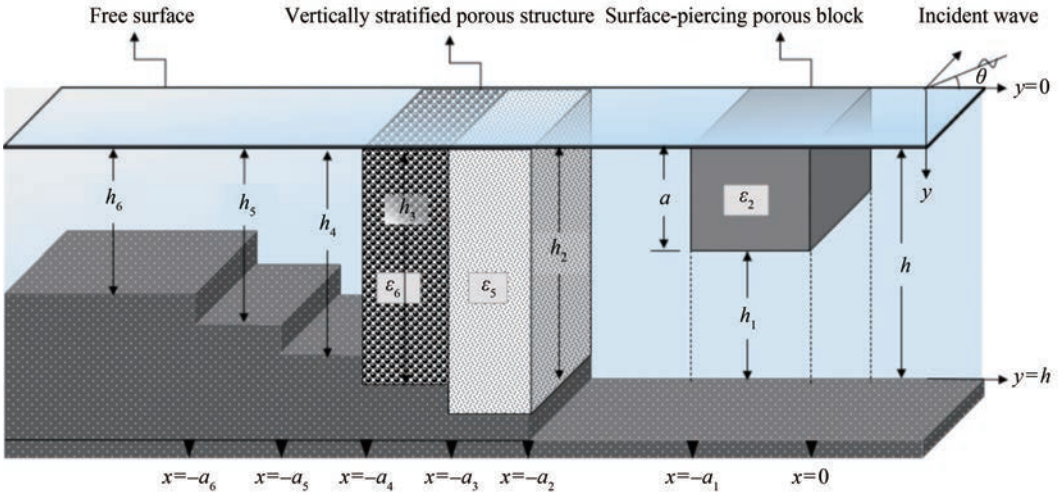

Figure 2 Vertically stratified porous structure with porous block in stepped seabed

$$\frac{\partial \phi_j}{\partial y} + K_j \phi_j = 0, \text{ on } y = 0 \tag{2}$$

where $K_{j=1,4,7,8,9} = \frac{\omega^2}{g}$, and $K_{j=5,6} = \frac{\omega^2}{g}\left(S_j + \mathrm{i}f_j\right)$ for free surface and vertically stratified porous structure region, S_j and f_j are reactance and frictional coefficients of porous regions of breakwater and g is the acceleration due to gravity. The bottom boundary condition due to the presence of impermeable sea-bed is given by

$$\frac{\partial \phi_j}{\partial y} = 0, \text{ on } y = h \tag{3}$$

The wave propagating due to the presence of the porous structure suggest the continuity of fluid pressure and velocity across the seaward and leeward structural interfaces. The linearized resistance f_j and reactance coefficients S_j (Sollitt and Cross, 1972) offered by each of the porous layer is determined on solving the relation given by

$$S_j = 1 + C_m\left[\frac{1-\varepsilon_j}{\varepsilon_j}\right], \text{ on } j = 2, 3 \tag{4a}$$

$$f_j = \frac{1}{\omega}\left\{\frac{\int_V \mathrm{d}V \int_t^{t+T} \varepsilon_j^2\left(\frac{\nu q^2}{\Lambda_p} + \frac{C_f \varepsilon_j}{\sqrt{\Lambda_p}}|q|^3\right)\mathrm{d}t}{\int_V \mathrm{d}V \int_t^{t+T} \varepsilon_j q^2 \mathrm{d}t}\right\}, \text{ on } j = 5, 6 \tag{4b}$$

where, C_m is coefficient of added mass considered to be very minimal/zero (Sollitt and Cross, 1972), thus $S_j = 1$ is kept fixed throughout the study. Λ_p is the intrinsic permeability, q the instantaneous Eulerian velocity vector, ν the kinematic viscosity, V the volume, C_f the turbulent resistant coefficient and T the wave period. The continuity of the velocity and pressure is satisfied for both surface piercing porous block and stratified porous structures. In the far-field region, the radiation conditions in the presence of porous structure is given by

$$\phi_{j=1,9}(x,y) = \begin{cases} \left(I_{10}\mathrm{e}^{-\mathrm{i}\gamma_{10}x} + R_{10}\mathrm{e}^{\mathrm{i}\gamma_{10}x}\right) f_{10}(y) & \text{as } x \to \infty \\ \left(T_{90}\mathrm{e}^{-\mathrm{i}\gamma_{30}x}\right) f_{90}(y) & \text{as } x \to -\infty \end{cases} \tag{5}$$

where, I_{10}, R_{10} and T_{90} are the complex amplitude of the incident, reflected and transmitted wave energies respectively. In the present study, the incident wave I_{10} is considered to be unity. The continuity of pressure and velocity due to the presence of surface piercing porous block at the edge $x = 0, -a_1$ and $j = 1, 4$ are given by

$$\phi_j(x,y)\Big|_{j=1,4} = \begin{cases} (S_2 + \mathrm{i}f_2)\phi_2(x,y) & \text{for } 0 < y < a \\ \phi_3(x,y) & \text{for } a < y < h \end{cases} \tag{6a}$$

$$\frac{\partial \phi_j(x,y)}{\partial x}\Big|_{j=1,4} = \begin{cases} \varepsilon_2 \frac{\partial \phi_2(x,y)}{\partial x} & \text{for } 0 < y < a \\ \frac{\partial \phi_3(x,y)}{\partial x} & \text{for } a < y < h \end{cases} \tag{6b}$$

The wave number in surface-piercing porous block region satisfies the dispersion relation for finite water depth given by

$$\omega^2 - g\gamma_{2n}\tanh\gamma_{2n}h - F_n\left[\omega^2\tanh\gamma_{2n}h - g\gamma_{2n}\right] = 0 \quad \text{for } n = 0, 1, 2, \cdots \tag{7a}$$

where,

$$F_n = \frac{\{(S_2 + \mathrm{i}f_2) - \varepsilon_2\}\tanh\gamma_{2n}a}{\{(S_2 + \mathrm{i}f_2) - \varepsilon_2\tanh^2\gamma_{2n}a\}} \tag{7b}$$

In Eq. 7(a), $\gamma_{2n}, n = 0, 1, 2, \cdots$ are the wave number for the surface-piercing porous block region which has infinite number of complex roots with the associated eigen value. The real part of the complex wave number, specifies the spatial periodicity (Sollitt and Cross, 1972) whereas the imaginary part specifies the decay rate. The dispersion relation due to the presence of surface-piercing block in Eq. 7(a) is solved using the perturbation method as discussed in Mendez and Losada (2004). The contour plot to determine the location of complex roots of the dispersion relation is presented in Figure 3 considering $S_2 = 1.0$, $f_2 = 0.5$, $a/h = 0.20$ and $\varepsilon_2 = 0.25$. The contour plots are used to find the initial guess for the determination of the roots of the dispersion relations.

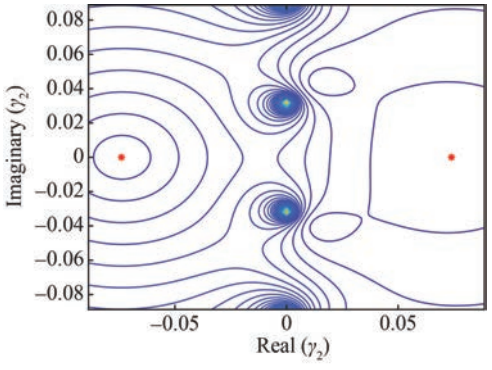

Figure 3 Contour plots of roots of dispersion relation of surface-piercing porous block considering $S_2 = 1.0$, $f_2 = 0.5$, $a/h = 0.20$ and $\varepsilon_2 = 0.25$

2.1 Horizontally stratified porous structure

The horizontally stratified porous structure is assumed to be placed at $-a_3 < x < -a_2$ on the leeward side of porous block over a rigid step and the water depth $0 < y < h_2$. So, the continuity of pressure and velocity due to the presence of two layered porous structure at the edge $x = -a_2, -a_3$ and $j = 4, 7$ are given by

$$\phi_j(x,y)\Big|_{j=4,7} = \begin{cases} (S_5 + \mathrm{i}f_5)\phi_5(x,y) & \text{for } 0 < y < b \\ (S_6 + \mathrm{i}f_6)\phi_6(x,y) & \text{for } b < y < h_2 \end{cases} \tag{8a}$$

$$\frac{\partial\phi_j(x,y)}{\partial x}\Big|_{j=4,7} = \begin{cases} \varepsilon_5\dfrac{\partial\phi_5(x,y)}{\partial x} & \text{for } 0 < y < b \\ \varepsilon_6\dfrac{\partial\phi_6(x,y)}{\partial x} & \text{for } b < y < h_2 \end{cases} \tag{8b}$$

In addition, there exists a flow within the surface and bottom porous layers in the vertical direction (Liu et al., 2007) for $-a_3 < x < -a_2$ and $y = b$ is given by

$$(S_5 + \mathrm{i}f_5)\phi_5(x,y) = (S_6 + \mathrm{i}f_6)\phi_6(x,y) \tag{9a}$$

$$\varepsilon_5\frac{\partial\phi_5(x,y)}{\partial y} = \varepsilon_6\frac{\partial\phi_6(x,y)}{\partial y} \tag{9b}$$

In the case of change in the bottom topography, the flow near rigid step at $x = -a_2, -a_3, -a_4, -a_5$ satisfies the zero-flow condition given by

$$\frac{\partial\phi_4(x,y)}{\partial x} = 0, \text{ for } h_2 < y < h$$
$$\frac{\partial\phi_6(x,y)}{\partial x} = 0, \text{ for } h_3 < y < h_2 \tag{10a}$$

$$\frac{\partial\phi_7(x,y)}{\partial x} = 0, \text{ for } h_4 < y < h_3$$
$$\frac{\partial\phi_8(x,y)}{\partial x} = 0, \text{ for } h_5 < y < h_4 \tag{10b}$$

The wave number in upstream/downstream free-water region γ_{j0} for $j = 1, 4, 7, 8, 9$ and porous structure region γ_{50} satisfies the dispersion relation for finite water depth is given by

$$\omega^2 = \begin{cases} g\gamma_{j0}\tanh\gamma_{j0}h_j & \text{for } n = 0 \\ -g\gamma_{jn}\tan\gamma_{jn}h_j & \text{for } n = 1, 2, \cdots \end{cases} \text{for } j = 1, 4, 7, 8, 9 \tag{11a}$$

$$(S_5 + \mathrm{i}f_5)\omega^2 - g\gamma_{5n}\tanh\gamma_{5n}h_2 = P_n\left[(S_5 + \mathrm{i}f_5)\omega^2\tanh\gamma_{5n}h_2 - g\gamma_{5n}\right] \quad \text{for } j = 5, n = 0, 1, 2, \cdots \tag{11b}$$

where, $h_j = h$ for $j = 1, 4$, $h_j = h_3$ for $j = 7$, $h_j = h_4$ for $j = 8$ and $h_j = h_5$ for $j = 9$ respectively with

$$P_n = \frac{\left\{1 - \dfrac{\varepsilon_6(S_5 + \mathrm{i}f_5)}{\varepsilon_5(S_5 + \mathrm{i}f_5)}\right\}\tanh\gamma_{5n}b}{\left\{1 - \dfrac{\varepsilon_6(S_5 + \mathrm{i}f_5)}{\varepsilon_5(S_6 + \mathrm{i}f_6)}\tanh^2\gamma_{5n}b\right\}} \tag{11c}$$

The dispersion relation of open water regions has one real root and infinite imaginary roots which is solved using Newton-Raphson method while the dispersion relation for horizontally stratified porous structure is having infinite number of complex roots which is solved using perturbation method (Mendez and Losada, 2004).

2.2 Vertically stratified porous structure

The vertically stratified porous structure is assumed to be placed at $-a_4 \leqslant x \leqslant -a_2$ over two rigid steps with water depths $0 \leqslant y \leqslant h_2$ and $0 < y < h_3$. So, the continuity of pressure and velocity due to the presence of two layered porous structure at the edges $x = -a_2, -a_3, -a_4$ are given by

$$\phi_4(x,y) = (S_5 + \mathrm{i}f_5)\phi_5(x,y) \text{ and}$$
$$\frac{\partial \phi_4(x,y)}{\partial x} = \varepsilon_5 \frac{\partial \phi_5(x,y)}{\partial x} \text{ at } x = -a_2 \tag{12a}$$

$$(S_5 + \mathrm{i}f_5)\phi_5(x,y) = (S_6 + \mathrm{i}f_6)\phi_6(x,y) \text{ and}$$
$$\varepsilon_5 \frac{\partial \phi_5(x,y)}{\partial x} = \varepsilon_6 \frac{\partial \phi_6(x,y)}{\partial x} \text{ at } x = -a_3 \tag{12b}$$

$$(S_6 + \mathrm{i}f_6)\phi_6(x,y) = \phi_7(x,y) \text{ and}$$
$$\varepsilon_6 \frac{\partial \phi_6(x,y)}{\partial x} = \frac{\partial \phi_7(x,y)}{\partial x} \text{ at } x = -a_4 \tag{12c}$$

In the case of vertically stratified porous structure, zero flow condition exists at the interface of rigid steps $x = -a_2, -a_3, -a_4, -a_5, -a_6$ given by

$$\frac{\partial \phi_4(x,y)}{\partial x} = 0, \text{ for } h_2 < y < h,$$
$$\frac{\partial \phi_5(x,y)}{\partial x} = 0, \text{ for } h_3 < y < h_2 \tag{13a}$$

$$\frac{\partial \phi_6(x,y)}{\partial x} = 0, \text{ for } h_4 < y < h_3,$$
$$\frac{\partial \phi_7(x,y)}{\partial x} = 0, \text{ for } h_5 < y < h_4 \tag{13b}$$

$$\frac{\partial \phi_8(x,y)}{\partial x} = 0, \text{ for } h_6 < y < h_5 \tag{13c}$$

The wave numbers in the upstream/downstream free-water regions are same as Eq. (11a) and the vertically stratified porous structure region satisfy the dispersion relation given by

$$\omega^2(S_j + \mathrm{i}f_j) = g\gamma_{jn} \tanh \gamma_{jn} h_j \text{ for } n = 0, 1, 2, \cdots \tag{14}$$

where $h_j = h_2, h_3$ for $j = 5, 6$ respectively. The dispersion relation for the vertically stratified porous structure region is solved using perturbation method (Mendez and Losada, 2004). The contour plot to determine the location of complex roots of the dispersion relation is presented in Figure 4.

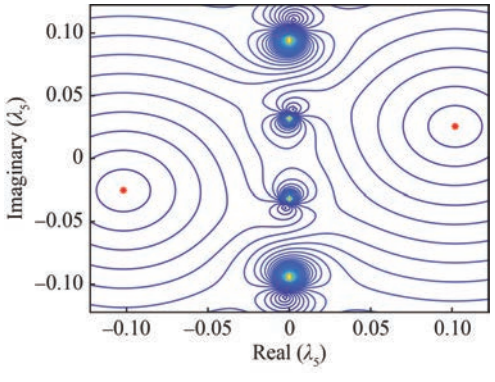

Figure 4 Contour plots of roots of dispersion relation of vertically stratified porous structure considering $S_5 = 1.0$, $f_5 = 0.25$ and $h_s/h = 0.50$

3 Method of solution for stratified structure with porous block

The wave interaction with the stratified porous structures combined with porous block in the presence of elevated sea-bed is examined using the eigenfunction expansion method. In the present section, the solution approach for both horizontally and vertically stratified porous structure is presented in detail. The velocity potential in the incident open water region for both the horizontally and vertically stratified structure over stepped seabed is given by

$$\phi_1(x,y) = \left(I_{10}\mathrm{e}^{-\mathrm{i}k_{10}x} + R_{10}\mathrm{e}^{\mathrm{i}k_{10}x}\right) f_{10}(y)$$
$$+ \sum_{n=1}^{\infty} R_{1n}\,\mathrm{e}^{-\mathrm{i}k_{1n}x} f_{1n}(y) \text{ for } 0 \leqslant x \leqslant \infty, 0 \leqslant y \leqslant h \tag{15}$$

where, I_{10} is the amplitude of the incident wave, R_{1n} for $n = 1, 2, 3, \cdots$ are the unknown constants to be determined. The vertical eigenfunction for incident open water region is given by

$$f_{1n}(y) = \begin{cases} \dfrac{\cosh \gamma_{10}(h-y)}{\cosh \gamma_{10} h} & \text{for } n = 0 \\ \dfrac{\cos \gamma_{1n}(h-y)}{\cos \gamma_{1n} h} & \text{for } n = 1, 2, \cdots \end{cases} \tag{16}$$

The velocity potential due to the presence of surface piercing porous block and leeward open water region are given by

$$\phi_2(x,y) = \sum_{n=0}^{\infty} \left\{A_{2n}\mathrm{e}^{-\mathrm{i}k_{2n}x} + B_{2n}\mathrm{e}^{\mathrm{i}k_{2n}(x+a_1)}\right\} f_{2n}(y),$$
$$-a_1 \leqslant x \leqslant 0, \quad 0 \leqslant y \leqslant a \tag{17a}$$

$$\phi_3(x,y) = \sum_{n=0}^{\infty} \left\{A_{2n}\mathrm{e}^{-\mathrm{i}k_{2n}x} + B_{2n}\mathrm{e}^{\mathrm{i}k_{2n}(x+a_1)}\right\} f_{3n}(y),$$
$$-a_1 \leqslant x \leqslant 0, \quad a \leqslant y \leqslant h \tag{17b}$$

$$\phi_4(x,y) = \left\{A_{40}\mathrm{e}^{-\mathrm{i}k_{j0}(x+a_{j-3})} + B_{40}\mathrm{e}^{\mathrm{i}k_{j0}(x+a_{j-2})}\right\} f_{40}(y)$$
$$+ \sum_{n=1}^{\infty} \left\{A_{4n}\mathrm{e}^{-\mathrm{i}k_{jn}(x+a_{j-3})} + B_{4n}\mathrm{e}^{\mathrm{i}k_{jn}(x+a_{j-2})}\right\} f_{4n}(y) \tag{17c}$$
$$-a_2 \leqslant x \leqslant -a_1, \quad 0 \leqslant y \leqslant h$$

where $A_{2n}, B_{2n}, A_{40}, B_{40}, A_{4n}, B_{4n}$ for $n = 0, 1, 2, \cdots$ are the unknown constants to be determined, $w_1 = a_1$ is thickness of the porous block. The vertical eigenfunctions for the porous block and leeward open water regions are given by

$$f_{2n}(y) = \frac{\cosh \gamma_{2n}(h-y) - F_n \sinh \gamma_{2n}(h-y)}{\cosh \gamma_{2n} h - F_n \sinh \gamma_{2n} h} \tag{18a}$$

$$f_{3n}(y) = \frac{1 - F_n \tanh\gamma_{2n} a \cosh\gamma_{2n}(h-y)}{(S_2 + \mathrm{i}f_2)(\cosh\gamma_{2n}h - F_n \sinh\gamma_{2n}h)}, \quad \text{for } n = 0, 1, 2, \cdots \tag{18b}$$

$$f_{4n}(y) = \begin{cases} \dfrac{\cosh\gamma_{40}(h-y)}{\cosh\gamma_{40}h} & \text{for } n = 0 \\ \dfrac{\cos\gamma_{4n}(h-y)}{\cos\gamma_{4n}h} & \text{for } n = 1, 2, \cdots \end{cases} \tag{18c}$$

The eigenfunctions $f_{jn}(y)$ for $j = 2, 3$ satisfy the orthogonal mode-coupling relation of the form

$$\left\langle f_{jn}, f_{jm} \right\rangle_{j=2,3} = \int_0^h f_{jn}(y) f_{jm}(y)\mathrm{d}y = \int_0^a f_{2n}(y) f_{2m}(y)\mathrm{d}y + \int_a^h f_{3n}(y) f_{3m}(y)\mathrm{d}y \tag{19}$$

Using the continuity of pressure and velocity along with orthogonal mode-coupling relation at the interface $x = 0, -a_1$, the equation is given by

$$\begin{aligned} \left\langle \phi_j(x,y), f_{jm}(y) \right\rangle_{j=1,4} &= \int_0^h \phi_j(x,y) f_{jm}(y)\mathrm{d}y \\ &= \left\{ \int_0^a + \int_a^h \right\} \phi_j(x,y) f_{jm}(y)\mathrm{d}y \\ &= (S_2 + \mathrm{i}f_2) \int_0^a \phi_2(x,y) f_{jm}(y)\mathrm{d}y \\ &+ \int_a^h \phi_3(x,y) f_{jm}(y)\mathrm{d}y \text{ for } m = 0, 1, 2, \cdots \end{aligned} \tag{20a}$$

$$\begin{aligned} \left\langle \phi_{jx}(x,y), f_{jm}(y) \right\rangle_{j=1,4} &= \int_0^h \phi_{jx}(x,y) f_{jm}(y)\mathrm{d}y \\ &= \left\{ \int_0^a + \int_a^h \right\} \phi_{jx}(x,y) f_{jm}(y)\mathrm{d}y \\ &= \varepsilon_2 \int_0^a \phi_2(x,y) f_{jm}(y)\mathrm{d}y \\ &+ \int_a^h \phi_3(x,y) f_{jm}(y)\mathrm{d}y \text{ for } m = 0, 1, 2, \cdots \end{aligned} \tag{20b}$$

3.1 Horizontally stratified porous structure

The velocity potentials due the presence of horizontally stratified porous structure and leeward open water regions are given by

$$\begin{aligned} \phi_j(x,y)\Big|_{j=5,6} &= \sum_{n=0}^{\infty} \left\{ A_{jn} \mathrm{e}^{-\mathrm{i}k_{jn}(x + a_{j-3})} + B_{jn} \mathrm{e}^{\mathrm{i}k_{jn}(x + a_{j-2})} \right\} f_{jn}(y) \\ &0 \leqslant y \leqslant b \text{ for } j = 5, b \leqslant y \leqslant h_2 \text{ for } j = 6 \end{aligned} \tag{21a}$$

$$\begin{aligned} \phi_j(x,y)\Big|_{j=7,8} &= \left\{ A_{j0} \mathrm{e}^{-\mathrm{i}k_{j0}(x + a_{j-3})} + B_{j0} \mathrm{e}^{\mathrm{i}k_{j0}(x + a_{j-2})} \right\} f_{j0}(y) \\ &+ \sum_{n=1}^{\infty} \left\{ A_{jn} \mathrm{e}^{-\mathrm{i}k_{jn}(x + a_{j-3})} + B_{jn} \mathrm{e}^{\mathrm{i}k_{jn}(x + a_{j-2})} \right\} f_{jn}(y), \\ &0 \leqslant y \leqslant h_3 \text{ for } j = 7, 0 \leqslant y \leqslant h_4 \text{ for } j = 8 \end{aligned} \tag{21b}$$

$$\phi_9(x,y) = T_{90} \mathrm{e}^{-\mathrm{i}k_{90}(x + a_5)} f_{90}(y) + \sum_{n=1}^{\infty} T_{9n} \mathrm{e}^{k_{9n}(x + a_5)} f_{9n}(y), \; -\infty \leqslant x \leqslant -a_5, \; 0 \leqslant y \leqslant h_5 \tag{21c}$$

where T_{90} is the transmitted wave amplitude, A_{jn}, B_{jn} and T_{9n} for $n = 0, 1, 2, \cdots$ and $j = 5, 6, 7, 8$ are the unknown constants to be determined, $w_2 = (a_3 - a_2)$ is thickness of the porous structure. The vertical eigenfunctions for the porous structure and leeward open water regions are given by

$$f_{5n}(y) = \frac{\cosh\gamma_{5n}(h_2 - y) - P_n \sinh\gamma_{5n}(h_2 - y)}{\cosh\gamma_{5n}h_2 - P_n \sinh\gamma_{5n}h_2} \tag{22a}$$

$$f_{6n}(y) = \frac{(S_5 + \mathrm{i}f_5)(1 - P_n \tanh(\gamma_{5n}b)\cosh\gamma_{5n}(h_2 - y))}{(S_6 + \mathrm{i}f_6)(\cosh\gamma_{5n}h_2 - P_n \sinh\gamma_{5n}h_2)}, \quad \text{for } n = 0, 1, 2, \cdots \tag{22b}$$

$$f_{jn}(y) = \begin{cases} \dfrac{\cosh\gamma_{j0}(h' - y)}{\cosh\gamma_{j0}h'} & \text{for } n = 0 \\ \dfrac{\cos\gamma_{jn}(h' - y)}{\cos\gamma_{jn}h'} & \text{for } n = 1, 2, \cdots \end{cases} \tag{22c}$$

where, $h' = h_3, h_4, h_5$ for $j = 7, 8, 9$ respectively. The eigenfunctions $f_{jn}(y)$ for $j = 1, 4, 7, 8, 9$ satisfy the orthogonal mode-coupling relation of the form

$$\left\langle f_{jn}, f_{jm} \right\rangle_{j=1,4,7,8,9} = \begin{cases} 0 & \text{for } m \neq n \\ C'_{jn} & \text{for } m = n \end{cases} \tag{23a}$$

$$\left\langle f_{jn}, f_{jm} \right\rangle_{j=5,6} = \int_0^{h_2} f_{jn}(y) f_{jm}(y)\mathrm{d}y = \int_0^b f_{5n}(y) f_{5m}(y)\mathrm{d}y + \int_b^h f_{6n}(y) f_{6m}(y)\mathrm{d}y \tag{23b}$$

where $C'_{jn} = \left\{ \dfrac{2\gamma_{jn}h_j + \sinh 2\gamma_{jn}h_j}{4\gamma_{jn}\cosh^2\gamma_{jn}h_j} \right\}$, for $j = 1, 4, 7, 8, 9, n = 0$ respectively with $C'_{jn}\Big|_{j=1,4,7,8,9}$ for $n = 1, 2, 3, \cdots$ are obtained by substituting $\gamma_{jn} = \mathrm{i}\gamma_{jn}$ in the case of open water region. Using the continuity of pressure and velocity along with orthogonal mode-coupling relation at the interface $x = -a_2, -a_3$, the equation is given by

$$\begin{aligned}\left\langle \phi_j(x,y), f_{jm}(y)\right\rangle_{j=4,7} &= \int_0^{h_2} \phi_j(x,y)\, f_{jm}(y)\,\mathrm{d}y \\ &= \left\{\int_0^b + \int_b^{h_2}\right\} \phi_j(x,y)\, f_{jm}(y)\,\mathrm{d}y \\ &= (S_5 + \mathrm{i}f_5)\int_0^b \phi_5(x,y)\, f_{jm}(y)\,\mathrm{d}y \\ &+ (S_6 + \mathrm{i}f_6)\int_b^{h_2} \phi_6(x,y)\, f_{jm}(y)\,\mathrm{d}y \text{ for } m = 0, 1, 2, \cdots\end{aligned} \tag{24a}$$

$$\begin{aligned}\left\langle \phi_{jx}(x,y), f_{jm}(y)\right\rangle_{j=4,7} &= \int_0^{h_2} \phi_{jx}(x,y)\, f_{jm}(y)\,\mathrm{d}y \\ &= \left\{\int_0^b + \int_b^{h}\right\} \phi_{jx}(x,y)\, f_{jm}(y)\,\mathrm{d}y \\ &= \varepsilon_5\int_0^b \phi_5(x,y)\, f_{jm}(y)\,\mathrm{d}y \\ &+ \varepsilon_6\int_b^{h_2} \phi_6(x,y)\, f_{jm}(y)\,\mathrm{d}y \text{ for } m = 0, 1, 2, \cdots\end{aligned} \tag{24b}$$

Next, the continuity of pressure and velocity at the edge $x = -a_4$ along with orthogonal mode-coupling relation is utilized to obtain the equation given by

$$\begin{aligned}\left\langle \phi_j(x,y), f_{jm}(y)\right\rangle_{j=7} &= \int_0^{h_3} \phi_7(x,y)\, f_{jm}(y)\,\mathrm{d}y \\ &= \int_0^{h_4} \phi_8(x,y)\, f_{jm}(y)\,\mathrm{d}y \text{ for } x = -a_4, m = 0, 1, 2, \cdots\end{aligned} \tag{25a}$$

$$\begin{aligned}\left\langle \phi_{jx}(x,y), f_{jm}(y)\right\rangle_{j=7} &= \int_0^{h_3} \phi_{7x}(x,y)\, f_{jm}(y)\,\mathrm{d}y \\ &= \int_0^{h_4} \phi_{8x}(x,y)\, f_{jm}(y)\,\mathrm{d}y \text{ for } x = -a_4, m = 0, 1, 2, \cdots\end{aligned} \tag{25b}$$

Further, the continuity of pressure and velocity at the edge $x = -a_5$ along with orthogonal mode-coupling relation is utilized to obtain the equation given by

$$\begin{aligned}\left\langle \phi_j(x,y), f_{jm}(y)\right\rangle_{j=8} &= \int_0^{h_4} \phi_8(x,y)\, f_{jm}(y)\,\mathrm{d}y \\ &= \int_0^{h_5} \phi_9(x,y)\, f_{jm}(y)\,\mathrm{d}y \text{ for } x = -a_5, m = 0, 1, 2, \cdots\end{aligned} \tag{26a}$$

$$\begin{aligned}\left\langle \phi_{jx}(x,y), f_{jm}(y)\right\rangle_{j=8} &= \int_0^{h_4} \phi_{8x}(x,y)\, f_{jm}(y)\,\mathrm{d}y \\ &= \int_0^{h_5} \phi_{9x}(x,y)\, f_{jm}(y)\,\mathrm{d}y \text{ for } x = -a_5, m = 0, 1, 2, \cdots\end{aligned} \tag{26b}$$

The infinite sums presented in the Eqs. 24(a–b), 25(a–b) and 26(a–b) obtained from the orthogonal mode-coupling relation are truncated upto finite M terms to obtain a linear system of $12(M+1)$ algebraic equations for the determination of $12(M+1)$ unknowns. The wave reflection and transmission coefficient due to the presence of porous structure is given by

$$K_r = \left|\frac{R_{10}}{I_{10}}\right| \text{ and } K_t = \left|\frac{T_{90}}{I_{10}}\right| \tag{27a}$$

Due the existence of porous structure along with stepped seabed the energy dissipation in the wave propagation is represented as

$$K_d = 1 - K_r^2 - \chi K_t^2 \tag{27b}$$

where $\chi = \left\{\frac{k_{j0}\tanh\gamma_{j0}h_j}{k_{10}\tanh\gamma_{10}h}\right\}\left\{\frac{\cosh^2\gamma_{10}h}{\cosh^2\gamma_{j0}h_j}\right\}\left\{\frac{2\gamma_{j0}h_j + \sinh 2\gamma_{j0}h_j}{2\gamma_{10}h + \sinh 2\gamma_{10}h}\right\}$.

In the next section, the wave attenuation due to the presence of vertically stratified porous structure is examined.

3.2 Vertically stratified porous structure

The velocity potentials in the porous structure and leeward open water regions for the vertically stratified porous structure are given by

$$\begin{aligned}\phi_j(x,y)\Big|_{j=5,6} &= \sum_{n=0}^{\infty}\left\{A_{jn}\mathrm{e}^{-\mathrm{i}k_{jn}(x+a_{j-3})} + B_{jn}\mathrm{e}^{\mathrm{i}k_{jn}(x+a_{j-2})}\right\} f_{jn}(y), \\ &0 \le y \le h_2 \text{ for } j = 5,\ 0 \le y \le h_3 \text{ for } j = 6\end{aligned} \tag{28a}$$

$$\begin{aligned}\phi_j(x,y)\Big|_{j=7,8} &= \left\{A_{j0}\mathrm{e}^{-\mathrm{i}k_{j0}(x+a_{j-3})} + B_{j0}\mathrm{e}^{\mathrm{i}k_{j0}(x+a_{j-2})}\right\} f_{40}(y) \\ &+ \sum_{n=1}^{\infty}\left\{A_{jn}\mathrm{e}^{-\mathrm{i}k_{jn}(x+a_{j-3})} + B_{jn}\mathrm{e}^{\mathrm{i}k_{jn}(x+a_{j-2})}\right\} f_{jn}(y), \\ &0 \le y \le h_4 \text{ for } j = 7,\ 0 \le y \le h_5 \text{ for } j = 8\end{aligned} \tag{28b}$$

$$\begin{aligned}\phi_9(x,y) &= T_{90}\mathrm{e}^{-\mathrm{i}k_{90}(x+a_6)} f_{90}(y) \\ &+ \sum_{n=1}^{\infty} T_{9n}\mathrm{e}^{k_{9n}(x+a_6)} f_{9n}(y), \text{ for } -\infty \le x \le -a_6,\ 0 \le y \le h_6\end{aligned} \tag{28c}$$

where T_{90} is the transmitted wave amplitude, A_{jn}, B_{jn} and T_{9n} for $j = 5, 6, 7, 8, n = 0, 1, 2, \cdots$ and are the unknown constants to be determined, $w_2 = (a_4 - a_2)$ is thickness of the porous structure. The vertical eigenfunctions for the porous structure and leeward open water regions are given by

$$f_{jn}(y) = \frac{\cosh\gamma_{jn}(h-y)}{\cosh\gamma_{jn}h} \text{ for } j = 5, 6, n = 0, 1, 2, \cdots \quad (29a)$$

$$f_{jn}(y)\Big|_{j=7,8,9} = \begin{cases} \dfrac{\cosh\gamma_{j0}(h_j - y)}{\cosh\gamma_{j0}h_j} & \text{for } n = 0 \\ \dfrac{\cos\gamma_{jn}(h_j - y)}{\cos\gamma_{jn}h_j} & \text{for } n = 1, 2, \cdots \end{cases} \quad (29b)$$

where, $h_j = h_4$ for $j = 7$, $h_j = h_5$ for $j = 8$ and $h_j = h_6$ for $j = 9$ respectively. The eigenfunctions $f_{jn}(y), j = 1, 4, 7, 8, 9$ satisfy the orthogonality relation of the form

$$\left\langle f_{jn}, f_{jm}\right\rangle_{j=1,4,7,8,9} = \begin{cases} 0 & \text{for } m \neq n, \\ C'_{jn} & \text{for } m = n, \end{cases} \text{and}$$

$$\left\langle f_{jn}, f_{jm}\right\rangle_{j=5,6} = \begin{cases} 0 & \text{for } m \neq n \\ C''_{jn} & \text{for } m = n \end{cases} \quad (30)$$

where $C'_n\Big|_{j=1,4,7,8,9} = \left\{\dfrac{2\gamma_{jn}h_j + \sinh 2\gamma_{jn}h_j}{4\gamma_{jn}\cosh^2\gamma_{jn}h_j}\right\}$, $n = 0$, and $C''_n\Big|_{j=5,6} = \left\{\dfrac{2\gamma_{jn}h + \sinh 2\gamma_{jn}h}{4\gamma_{jn}\cosh^2\gamma_{jn}h}\right\}$, $n = 0, 1, 2, \cdots$ with $C'_n\Big|_{j=1,4,7,8,9}$ for $n = 1, 2, 3, \cdots$ are obtained by substituting $\gamma_{jn} = \mathrm{i}\gamma_{jn}$ in the case of open water region.

Using the orthogonal mode-coupling relation at the interface $x = -a_2$, $0 \leqslant y \leqslant h_2$ we have

$$\left\langle \phi_4(x,y), f_{4m}(y)\right\rangle = \int_0^{h_2} \phi_4(x,y)\, f_{4m}(y)\,\mathrm{d}y = (S_5 + \mathrm{i}f_5)\int_0^{h_2} \phi_5(x,y)\, f_{4m}(y)\,\mathrm{d}y \text{ for } m = 0, 1, 2, \cdots \quad (31a)$$

$$\left\langle \phi_{4x}(x,y), f_{4m}(y)\right\rangle = \int_0^{h_2} \phi_{4x}(x,y)\, f_{4m}(y)\,\mathrm{d}y = \varepsilon_5\int_0^{h_2} \phi_{5x}(x,y)\, f_{4m}(y)\,\mathrm{d}y \text{ for } m = 0, 1, 2, \cdots \quad (31b)$$

Also, at the interface between the porous layers $x = -a_3$, $0 \leqslant y \leqslant h_2$, the continuity of pressure and the pressure and velocity along with orthogonal relation gives

$$\left\langle \phi_5(x,y), f_{5m}(y)\right\rangle = \int_0^{h_2} \phi_5(x,y)\, f_{5m}(y)\,\mathrm{d}y = \left\{\frac{S_6 + \mathrm{i}f_6}{S_5 + \mathrm{i}f_5}\right\}\int_0^{h_2} \phi_6(x,y)\, f_{5m}(y)\,\mathrm{d}y \text{ for } m = 0, 1, 2, \cdots \quad (32a)$$

$$\left\langle \phi_{5x}(x,y), f_{5m}(y)\right\rangle = \int_0^{h_2} \phi_{5x}(x,y)\, f_{5m}(y)\,\mathrm{d}y = \left\{\frac{\varepsilon_6}{\varepsilon_5}\right\}\int_0^{h_2} \phi_{6x}(x,y)\, f_{5m}(y)\,\mathrm{d}y \text{ for } m = 0, 1, 2, \cdots \quad (32b)$$

The continuity of pressure and velocity at the edge $x = -a_4$ along with orthogonal mode-coupling relation is utilized to obtain the equation given by

$$\left\langle \phi_7(x,y), f_{7m}(y)\right\rangle = \int_0^{h_4} \phi_7(x,y)\, f_{7m}(y)\,\mathrm{d}y = (S_6 + \mathrm{i}f_6)\int_0^{h_4} \phi_6(x,y)\, f_{7m}(y)\,\mathrm{d}y \text{ for } x = -a_4, m = 0, 1, 2, \cdots \quad (33a)$$

$$\left\langle \phi_{7x}(x,y), f_{7m}(y)\right\rangle = \int_0^{h_4} \phi_{7x}(x,y)\, f_{7m}(y)\,\mathrm{d}y = \varepsilon_6\int_0^{h_4} \phi_{6x}(x,y)\, f_{7m}(y)\,\mathrm{d}y \text{ for } x = -a_4, m = 0, 1, 2, \cdots \quad (33b)$$

Next, the continuity of pressure and velocity at the edge $x = -a_5$ along with orthogonal mode-coupling relation is utilized to obtain the equation given by

$$\left\langle \phi_j(x,y), f_{jm}(y)\right\rangle_{j=7} = \int_0^{h_4} \phi_7(x,y)\, f_{jm}(y)\,\mathrm{d}y = \int_0^{h_5} \phi_8(x,y)\, f_{jm}(y)\,\mathrm{d}y \text{ for } x = -a_5, m = 0, 1, 2, \cdots \quad (34a)$$

$$\left\langle \phi_{jx}(x,y), f_{jm}(y)\right\rangle_{j=7} = \int_0^{h_4} \phi_{7x}(x,y)\, f_{jm}(y)\,\mathrm{d}y = \int_0^{h_5} \phi_{8x}(x,y)\, f_{jm}(y)\,\mathrm{d}y \text{ for } x = -a_5, m = 0, 1, 2, \cdots \quad (34b)$$

Further, the continuity of pressure and velocity at the edge $x = -a_6$ along with orthogonal mode-coupling relation is utilized to obtain the equation given by

$$\left\langle \phi_j(x,y), f_{jm}(y)\right\rangle_{j=8} = \int_0^{h_5} \phi_8(x,y)\, f_{jm}(y)\,\mathrm{d}y = \int_0^{h_6} \phi_9(x,y)\, f_{jm}(y)\,\mathrm{d}y \text{ for } x = -a_6, m = 0, 1, 2, \cdots \quad (35a)$$

$$\left\langle \phi_{jx}(x,y), f_{jm}(y)\right\rangle_{j=8} = \int_0^{h_5} \phi_{8x}(x,y)\, f_{jm}(y)\,\mathrm{d}y = \int_0^{h_6} \phi_{9x}(x,y)\, f_{jm}(y)\,\mathrm{d}y \text{ for } x = -a_6, m = 0, 1, 2, \cdots \quad (35b)$$

The infinite sums presented in the Eqs. 31(a–b)–35(a–b) obtained from the orthogonal mode-coupling in open water regions are truncated upto finite M terms to obtain a linear system of $14(M + 1)$ algebraic equations for the determination of $14(M + 1)$ unknowns. The wave reflection, transmission and dissipation coefficients due to the presence of vertically stratified structure are same as in Eq. 27(a–b).

3.3 Wave force on the front face of porous block and stratified structure

The wave force impact acting on the front face of porous block, K_{fb1} and that of stratified structure, K_{fs1} are given by

$$K_{fb1} = \left| \frac{F_{fb1}}{2\rho g h I_{10}} \right| \text{ and } K_{fs1} = \left| \frac{F_{fs1}}{2\rho g h I_{10}} \right| \tag{36a}$$

and I_{10} is the amplitude of the incident wave potential considered to be unity. In the case of surface piercing porous block, F_{fb1} is given by

$$F_{fb1} = \mathrm{i}\rho\omega \int_0^a \left\{ \phi_2(x,y) - \phi_1(x,y) \right\} \mathrm{d}y \quad \text{at} \quad x = 0 \tag{36b}$$

In the case of horizontally stratified porous structure, F_{fs1} for $j = 5, 6$ is given by

$$F_{\mathrm{fs1}} = \mathrm{i}\rho\omega \left\{ \int_0^h \phi_j(x,y)\,\mathrm{d}y - \int_0^h \phi_4(x,y)\,\mathrm{d}y \right\} \quad \text{at} \quad x = -a_2 \tag{37a}$$

In the case of vertically stratified porous structure, F_{fs1} is given by

$$F_{\mathrm{fs1}} = \mathrm{i}\rho\omega \int_0^{h_2} \left\{ \phi_5(x,y) - \phi_4(x,y) \right\} \mathrm{d}y \text{ at } x = -a_2 \tag{37b}$$

3.4 Surface elevation

The free surface gravity wave elevation in the incident and transmitted wave regions are obtained from the relations

$$-\mathrm{i}\omega\zeta_j = \phi_{jy} \text{ on } y = 0, \ j = 1, 9 \tag{38a}$$

which can be expressed in the form as

$$\zeta_j(x) = \frac{\mathrm{i}}{\omega} \begin{cases} -\left(I_{10}\mathrm{e}^{-\mathrm{i}k_{10}x} + R_{10}\mathrm{e}^{\mathrm{i}k_{10}x} \right)\gamma_{10}\tanh\gamma_{10}h + \sum_{n=1}^{\infty} R_{1n}\mathrm{e}^{-\kappa_{1n}x}\gamma_{1n}\tan\gamma_{1n}h & \text{for } 0 < x < \infty \\ -T_{90}\mathrm{e}^{-\mathrm{i}k_{90}(x+a_j)}\gamma_{90}h_j + \sum_{n=1}^{\infty} T_{9n}\mathrm{e}^{\kappa_{9n}(x+a_j)}\gamma_{9n}\tan\gamma_{9n}h_j & \text{for } -\infty < x < -a_j \end{cases} \tag{38b}$$

where, $-a_j = -a_5$, $h_j = h_5$ for horizontally stratified structure and $-a_j = -a_6$, $h_j = h_6$ in the case of vertically stratified porous structure. The numerical investigation performed using the eigenfunction expansion method is for the regular geometry of the stratified porous structure and elevated sea-bed. In the case of irregular geometry, the numerical approach using the eigenfunction expansion method can be coupled with Boundary Element Method (BEM) to perform the numerical investigation.

4 Numerical results and discussion for stratified structure with porous block

The numerical investigation is performed to examine the wave interaction due to stratified porous structure combined with surface-piercing porous block in changing bottom topography considering various values of porosity ε, linearized friction factor f, angle of incidence θ, finite spacing between the structures and porous block L. The wave reflection K_r, transmission coefficient K_t, energy dissipation K_d, wave force impact on the front face of the porous block K_{fb1}, wave force impact on the front face of the stratified structure K_{fs1} and the surface deflection in the incident and transmitted region $\zeta_j(x)$ is plotted to understand the behaviour of porous structure with change in bottom topography for wave energy dissipation. The convergence study in K_r and K_t due to the increasing number of evanescent wave modes M is performed for horizontally and vertically stratified porous structure combined with a surface-piercing porous block placed on stepped sea bottom and the numerical results obtained are tabulated in Table 1. The numerical result is noted to converge with the increase in the number of evanescent wave modes $M \geqslant 15$ as tabulated in Table 1. In the present study the evanescent wave mode is truncated for $M = 15$ and the numerical results are evaluated. The parameters that are kept constant are $\rho = 1\,000$ kg/m^3, $g = 9.81$ m/s^2 and $S_j = 1$ throughout the computation.

4.1 Validation of the numerical model

The numerical modelling of single layered and multi-layered porous structures for different configurations is performed by Dattatri et al. (1978), Dalrymple et al. (1991), Zhu and Chwang (2001) and Liu and Li (2013). The study conducted on a single layer porous structure is validated with results from the literature in order to assess the validity of the present numerical model based on the eigenfunction expansion method. Dalrymple et al. (1991)

Table 1 Convergence of K_r and K_t for horizontally and vertically stratified porous structure combined with a surface-piercing porous block placed on stepped sea bottom considering $\gamma_{10}h = 1.5$, $w_1/h = 0.50$, $w_1/h = 0.50$, $L/h = 0.25$, $a/h = 0.25$, $\theta = 20°$, $S_2 = S_5 = S_6 = 1$, $\varepsilon_2 = 0.2$, $f_2 = 0.6$, $f_5 = 0.8$ and $f_6 = 0.5$

Evanescent modes M	Horizontally stratified porous structure with surface-piercing porous block		Vertically stratified porous structure with surface-piercing porous block	
	K_r	K_t	K_r	K_t
0	0.435 36	0.618 27	0.365 42	0.302 39
5	0.420 36	0.623 61	0.328 95	0.336 77
10	0.410 08	0.630 45	0.301 36	0.342 71
15	0.408 83	0.639 55	0.293 52	0.345 64
20	0.408 84	0.639 52	0.293 54	0.345 60

examined the reflection and transmission characteristics for oblique wave incidence on a vertical porous structure using plane wave approximation.

In Figure 5 the comparative study between the present numerical model and the results obtained for single porous structure on wave reflection coefficient for varying angle of incidence is performed and a good agreement with the result obtained by Dalrymple et al. (1991) is noted. The study reveals that, with the increase in the linearized friction factor, the minimum in the reflection coefficient is obtained for $65° < \theta < 75°$ Further, Liu and Li (2013) developed an analytical solution for wave reflection and transmission by a surface-piercing porous breakwater without using the complex dispersion relation. The results obtained for the reflection and transmission coefficient (Figure 6) based on the analytical solution of single layer porous structure as in Liu and Li (2013) is compared with that result obtained using the present numerical approach. The study shows a considerable agreement between the results using the present numerical approach and by Liu and Li (2013) for both reflection and transmission coefficients. Thereafter, the numerical investigation is extended for both horizontally and vertically stratified porous structure combined with porous block in varying seabed.

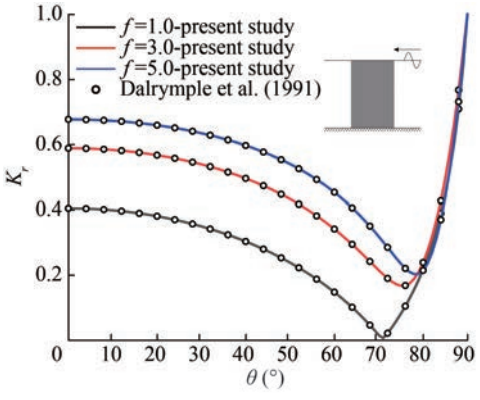

Figure 5 Comparative study for the reflection coefficient in the case of single porous structure and Dalrymple et al. (1991) considering $B/h = 1$, $\omega^2 h/g = 0.2012$, $S = 1$ and $\varepsilon = 0.45$

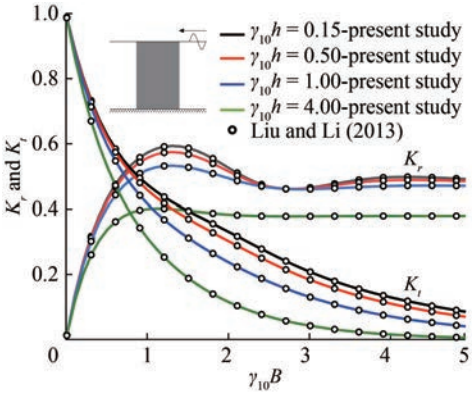

Figure 6 Comparative study for K_r and K_t using the present analytical approach for single porous structure and Liu and Li (2013) considering $\varepsilon = 0.45$, $S = 1$ and $f = 1$

4.2 Horizontally stratified porous structure with surface-piercing porous block

The wave transformation due to horizontally stratified porous structure combined with porous block in changing bottom topography is analyzed on studying the wave reflection coefficient K_r, transmission coefficient K_t, dissipation coefficient K_d, surface displacement $\zeta_j(x)$, wave force acting on the front face of porous block K_{fb1} and on the stratified structure K_{fs1}.

4.2.1 Reflection, transmission and dissipation coefficient

The wave reflection, transmission and dissipation coefficients are analysed for the change in the porosity, change in structural width, change in dimensionless wave number, change in the angle of incidence.

4.2.1.1 Effect of multiple porosities

In order to analyze the effect of porosity on hydrodynamic coefficients, the behaviour of combinations of different porosity for top and bottom porous layer of stratified structure is studied in Figure 7(a–b) for varying dimensionless width of structure. The stratified porous structure with uniform porosity of 50% is observed to have more wave reflection and intermediate transmission compared

to the other combinations. The wave reflection shows intermediate characteristics, and transmission coefficient is least for combination of $\varepsilon_5 = 0.7$ and $\varepsilon_6 = 0.3$. As a result, wave dissipation is higher for the porosity combination $\varepsilon_5 = 0.7$ and $\varepsilon_6 = 0.3$. A mono resonating behaviour is observed for K_r and maximum peak is observed when width of porous structure is same as the depth of incident open water region. The maximum wave reflection may be due to constructive inference between incident and reflected waves by the porous structure. Thus for $\varepsilon_5 = 0.7$ and $\varepsilon_6 = 0.3$, K_r for uniform porosity is 33.33% more than that of combination of $\varepsilon_5 = 0.9$ and $\varepsilon_6 = 0.1$. Most of the surface concentrated waves may be either attenuated or reflected by the surface-piercing porous block and hence only the remaining incoming wave energy are attenuated by the stratified structure.

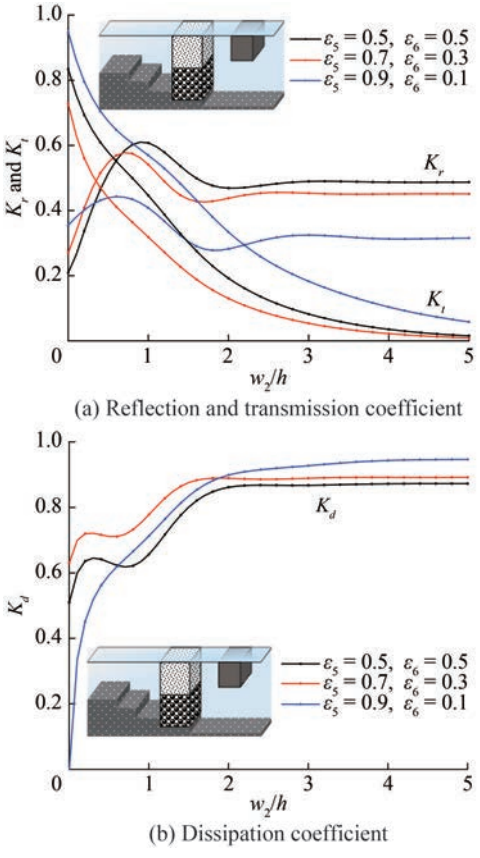

Figure 7 Variation of K_r, K_t and K_d versus w_2/h for different combinations of porosities considering $\gamma_{10}h = 1.5$, $h_s/h = 0.10$, $w_1/h = 0.50$, $L/h = 0.25$, $\theta = 20°$, $S_2 = S_5 = S_6 = 1$, $\varepsilon_2 = 0.2$, $f_2 = 0.6$, $f_5 = 0.8$ and $f_6 = 0.5$

In Figure 7(a), it can be noted that K_r is decreasing as the porosity of surface layer is increasing which may be caused due to the easy penetration of waves through the pores of surface layer of stratified structure. This is evident from K_t in Figure 7(a) that with the maximum wave transmission is observed for the combination of highest porosity at the surface layer. Further, about 95% wave energy dissipation is achieved when width of stratified structure is more than 1.5 times the water depth as depicted in Figure 7(b).

4.2.1.2 Effect of structural width of porous block and stratified structure

Figure 8 illustrates the hydrodynamic coefficients versus θ for different structural width of the porous block varying within $0.5 < w_1/h < 3.0$. The increase in the structural width w_1/h shows an increase in wave reflection but a decrease in wave transmission. For direct wave attack, K_r for $w_1/h = 3.0$ is observed to be twice as compared to $w_1/h = 0.5$. Also, a small mono resonating behaviour in K_r is prominent at $\theta = 22°$ as width of porous block increases. This can be due to the change in phase of the incident and reflected wave due to the increased width of the porous structure. For higher angle of incidence, a steep increase in wave reflection is observed.

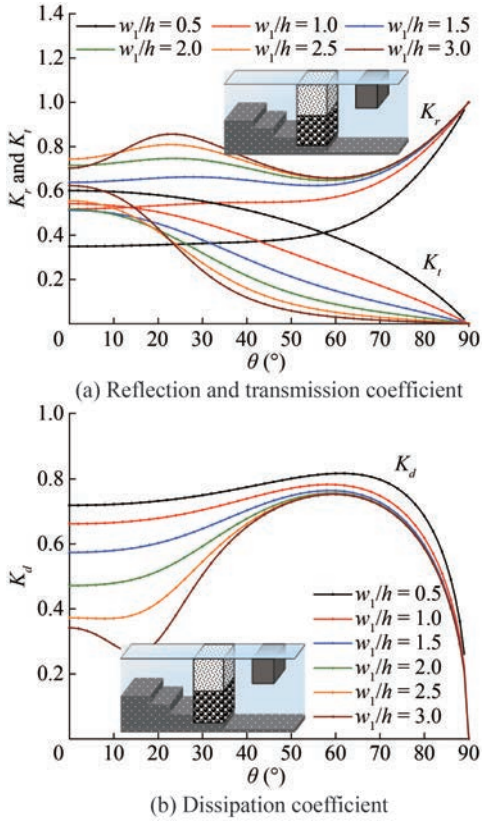

Figure 8 Variation of K_r, K_t and K_d versus θ for different values of w_1/h considering $\gamma_{10}h = 1.5$, $h_s/h = 0.10$, $a/h = 0.25$, $w_2/h = 0.50$, $L/h = 0.25$, $S_2 = S_5 = S_6 = 1$, $\varepsilon_2 = 0.2$, $\varepsilon_5 = 0.7$, $\varepsilon_6 = 0.4$, $f_2 = 0.6$, $f_5 = 0.8$ and $f_6 = 0.5$

As depicted in Figure 8(b), wave energy dissipation decreases with increase in width of porous block, although larger variation is not observed for oblique waves with angle of incidence greater than $\theta = 45°$. At $\theta = 15°$, K_d shows a decrease of 65.28% from $w_1/h = 0.5$ to $w_1/h = 3.0$. The decrease in wave energy dissipation is caused as most of

the incoming waves are being reflected by the porous block. A local minima is observed in K_d for w_1/h = 3.0 due to the sudden increase in wave reflection. A steep decrease in K_d is observed for higher angle of incidence which is an opposite trend to that of K_r. This may be due to the less effective wave trapping as most of this incoming wave energy is being reflected by the porous structure.

The hydrodynamic behaviour of structure with respect to different structural width of stratified porous structure as well is analysed for varying angle of incidence. In Figure 9(a) the variation in K_r is observed, which increases with more oblique wave angle. Also wave reflection is more when width of structure is half of the open water depth. In all other cases, no significant variation in K_r is observed. Wave transmission characteristics for w_2/h = 0.5 also suggests that this structural width is not suitable for stratified structure as K_t is more. This is due to the availability of shorter path through the stratified porous structure and hence lesser pore spaces for the wave energy to be dissipated. For θ = 0°, wave transmission decreases by around 82% when w_2/h is increased from 0.5 to 3.0. Wave damping efficiency for most cases, except for w_2/h = 0.5 is greater than 90% as noted in Figure 9(b). Since, for all other cases, wave damping efficiency is almost the same, it is economical to construct stratified porous structure with intermediate structural width and to decrease wave transmission for this width of stratified structure, it is better to increase the width of surface-piercing porous block. Thus, cost can be considerably reduced due to the combination of a fully extended structure with a partial porous structure.

4.2.1.3 Effect of dimensionless wavenumber

To examine the behaviour of waves in the presence of horizontal stratified structure combined with porous block in changing bottom topography the dimensionless wave number ranging from 0.75 to 1.75 is varied. In Figure 10, the wave reflection, transmission and dissipation coefficients are analysed for varying length between stratified structure and porous block with the change in the non-dimensional wave number. Due to high wave oscillations in the confined region, resonating behaviour is observed for the hydrodynamic coefficients which allow us to determine the optimum length to be provided between stratified structure and porous block from the resonating troughs. The minimum value in wave reflection as observed in Figure 10(a) corresponds to the destructive interference of the waves due to the presence of the porous block. It is observed that wave reflection for shorter waves is more compared to longer waves. Further, wave transmission for longer waves is more. This is due to the lesser interaction of longer waves compared to the length of the structure and vice versa for shorter waves. In addition, as represented in Figure 10(b), wave damping efficiency for shorter waves is higher for the structure, although more prominent resonating behaviour is observed for such waves. However, the oscillating

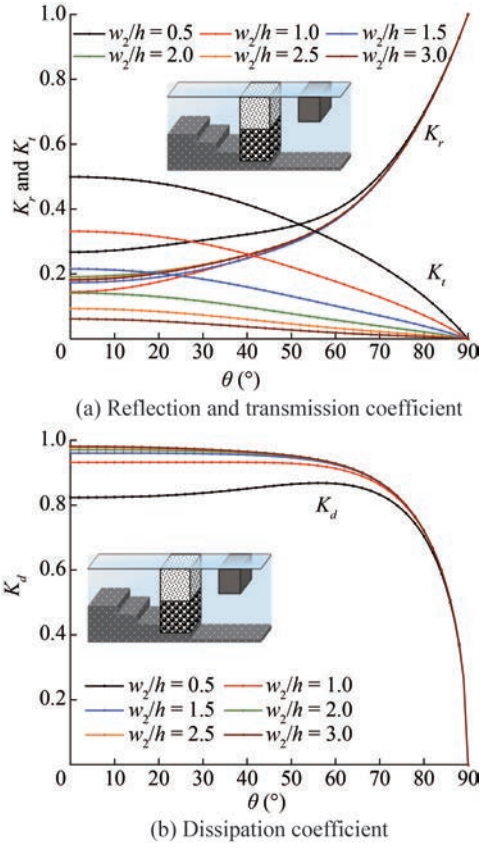

Figure 9 Variation of K_r, K_t and K_d versus θ for different values of w_2/h considering $\gamma_{10}h$ = 1.5, h_s/h = 0.10, a/h = 0.25, w_1/h = 0.50, L/h = 0.25, $S_2 = S_5 = S_6$ = 1, ε_2 = 0.2, ε_5 = 0.7, ε_6 = 0.4, f_2 = 0.6, f_5 = 0.8 and f_6 = 0.5

pattern diminishes for lesser value of $\gamma_{10}h$ and more uniform value is achieved due to the formation of the standing waves in the confined region formed by the porous block in seaward side and rigid steps in leeward side with the horizontally stratified structure.

In Figure 11 the effect of dimensionless wavenumber for varying dimensionless width of stratified structure is presented for varying dimensionless width of stratified structure. For shorter waves, wave reflection is more, and transmission is minimum compared to longer waves due to increased wave interaction with the structure as illustrated in Figure 11(a). In addition, as the width of stratified structure is increased, K_r achieves more consistent value and hence any further increase in width of structure has less effect on wave reflection characteristic. The local maxima observed in K_r for 0.5 < w_2/h < 1.5 may be caused due to the constructive interference between incoming and reflected waves. However, this local maximum value shifts towards left with the increase in $\gamma_{10}h$, which can be due to the change in phase of incident and reflected waves when the wavelength of incoming waves changes. Also, even for small structural width, wave dissipation behaviour for shorter waves is efficient as presented in Figure 11(b). A

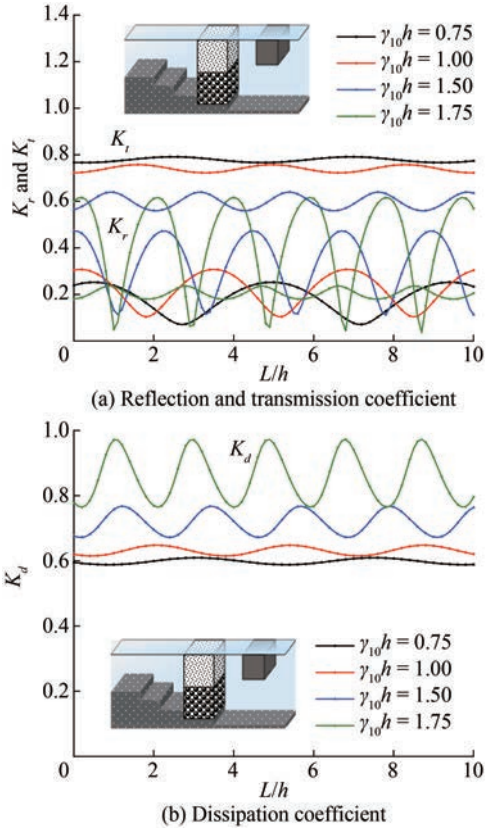

Figure 10 Variation of K_r, K_t and $K_d$versus L/h for different values of $\gamma_{10}h$ considering $h_s/h = 0.10$, $a/h = 0.25$, $w_1/h = w_2/h = 0.50$, $\theta = 20°$, $S_2 = S_5 = S_6 = 1$, $\varepsilon_2 = 0.2$, $\varepsilon_5 = 0.7$,$\varepsilon_6 = 0.3$, $f_2 = 0.6$, $f_5 = 0.8$ and $f_6 = 0.5$

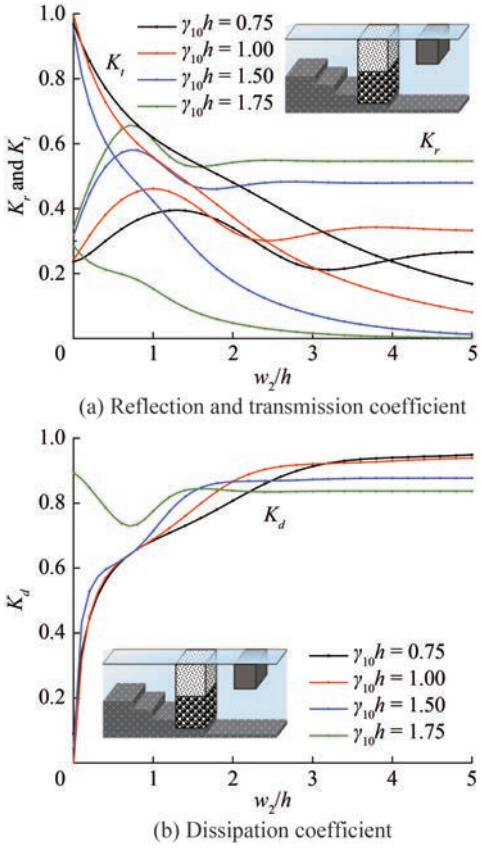

Figure 11 Variation of K_r, K_t and K_d versus w_2/h for different values of $\gamma_{10}h$ considering $h_s/h = 0.10$, $a/h = 0.25$, $w_1/h = 0.50$, $L/h = 0.25$, $\theta = 20°$, $S_2 = S_5 = S_6 = 1$, $\varepsilon_2 = 0.2$, $\varepsilon_5 = 0.7$, $\varepsilon_6 = 0.3$, $f_2 = 0.6$, $f_5 = 0.8$ and $f_6 = 0.5$

local minima is observed in the case of $\gamma_{10}h = 1.75$ because of high wave reflection on account of standing wave formation. Hence, this structure is economical for waves with shorter wavelength. In the case of an increased width of stratified structure, longer waves can also be attenuated effectively by better interaction of wave with structure.

4.2.1.4 Effect of angle of incidence

The impact of angle of wave attack on the wave transformation is examined for the stratified porous structure combined with porous block for stepped seabed. The hydrodynamic coefficients are studied varying angle of incidence within $0 \leqslant \theta \leqslant 90°$ in Figure 12(a–b) for different combinations of porosity of surface and bottom layers of stratified structure. It can be inferred from Figure 12(a) that, for more oblique waves, $\theta > 60°$, K_r increases considerably, whereas transmission decreases due to increased wave interaction with structure. Further, for higher angle of incidence, wave dissipation property of the structure as shown by Figure 12(b) decreases. This may be caused due to increased reflection, as a result of which only marginal number of waves would be passing through the porous structure and hence lesser wave energy attenuation of incoming waves.

4.2.1.5 Effect of length between porous block and stratified structure

The variation of hydrodynamic coefficients with the change in the length between porous block and the stratified structure for varying combination of porosity of surface and bottom porous layer is studied and presented in Figure 13. An oscillating pattern is obtained for all the cases of combinations of porosity. This oscillation diminishes as the porosity of surface layer is increased and that of bottom layer is decreased. This may be due to the formation of standing waves in the confined region between surface-piercing porous block and stratified structure. In addition, the trough is observed for L/h having the value 1.0, 3.0, 4.0 and so on. The L/h values are significant for designing the structure as we can achieve minimal wave reflection. In these cases, even zero wave reflection is observed in Figure 13(a). This may be the case when incident and reflected waves are 180° out of phase and all the waves are absorbed within the confined region. Also, reflection coefficient decreases as the porosity of surface layer is increased and the bottom layer is decreased. This is due to the availability of more pore spaces in surface layer to

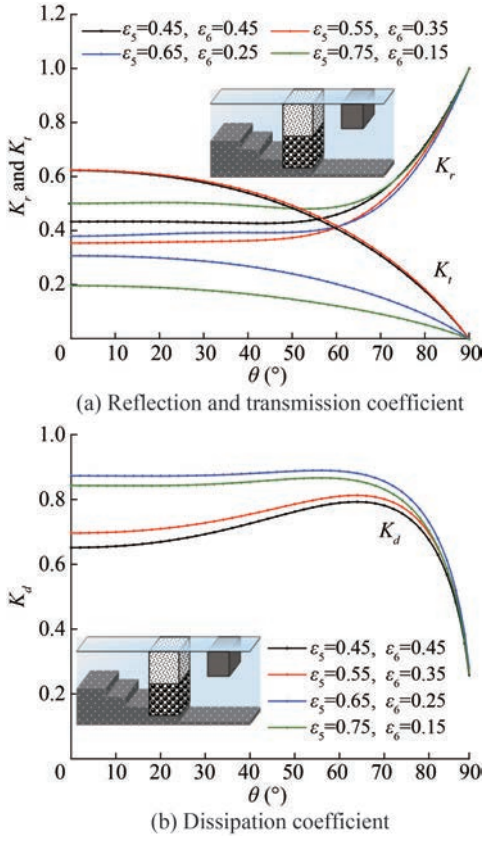

Figure 12 Variation of K_r, K_t and K_d versus θ for different combinations of porosities considering $\gamma_{10}h$ = 1.5, h_s/h = 0.10, a/h = 0.25, $w_1/h = w_2/h$ = 0.50, L/h = 0.25, $S_2 = S_5 = S_6$ = 1, ε_2 = 0.2, f_2 = 0.6, f_5 = 0.8 and f_6 = 0.5

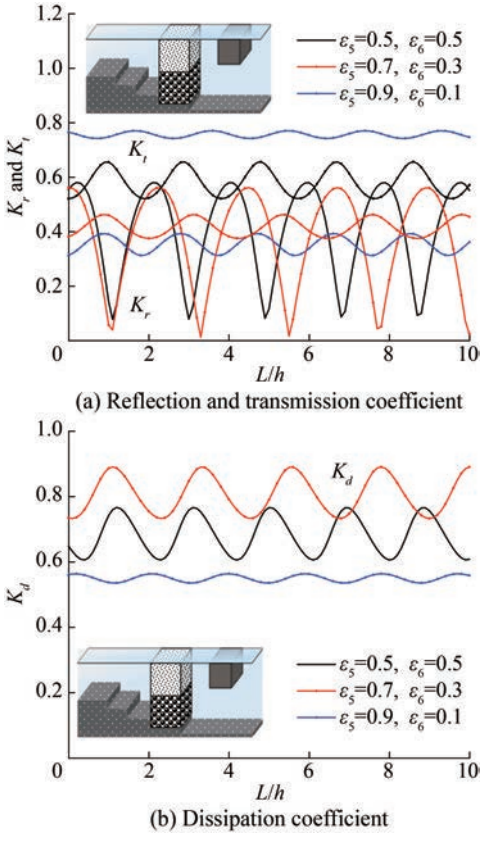

Figure 13 Variation of K_r, K_t and K_d versus L/h for different combinations of porosities considering $\gamma_{10}h$ = 1.5, h_s/h = 0.10, a/h = 0.25, $w_1/h = w_2/h$ = 0.50, θ = 20°, $S_2 = S_5 = S_6$ = 1, ε_2 = 0.2, f_2 = 0.6, f_5 = 0.8 and f_6 = 0.5

allow more surface waves to pass through. Resonating peaks are also observed in the case of K_t, such that the value is increasing with increase in porosity of surface layer. However, wave damping efficiency is maximum shown for the combination with $\varepsilon_5 = 0.7$ and $\varepsilon_6 = 0.3$. Resonating crests for K_d as depicted in Figure 13(b) are observed for L/h corresponding to negligible or fairly zero wave reflection due to the absorption of incoming wave energy.

4.2.2 Surface elevation

The surface elevation in the open water regions for various angle of incidence of gravity waves in the range $0 \leqslant \theta \leqslant 60°$ is analysed in Figure 14. The maximum surface elevation is observed in the case of θ = 60° for the incident open water region. However, irrespective of incident wave angle, considerable reduction in surface elevation of transmitted region is achieved due to the presence of the structure.

Most attenuation is achieved in the case of higher angle of incidence due to considerably more interaction of oblique waves with the structure. Phase change in the incoming waves is observed in Figure 14 due to the presence of the structure. Thus, it is clear that a tranquil zone can be created in the leeward side by the combination of stratified

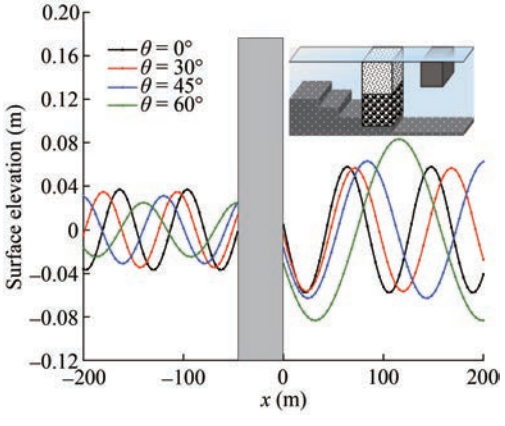

Figure 14 Surface elevation versus x for different values of θ considering $\gamma_{10}h$ = 1.5, h_s/h = 0.10, a/h = 0.25, $w_1/h = w_2/h$ = 0.50, L/h = 0.25, $S_2 = S_5 = S_6$ = 1, ε_2 = 0.2, ε_5 = 0.7, ε_6 = 0.3, f_2 = 0.6, f_5 = 0.8 and f_6 = 0.5

structure with surface-piercing porous block.

4.2.3 Wave force on front face of porous block and stratified structure

Figure 15 shows the force acting on front face of both

horizontally stratified porous structure and the surface piercing porous block varying dimensionless wavenumber. It is observed that K_{fs1} is less when longer waves are incident as noted in Figure 15(a) This is because longer waves have least interaction with structure and hence less reflection.

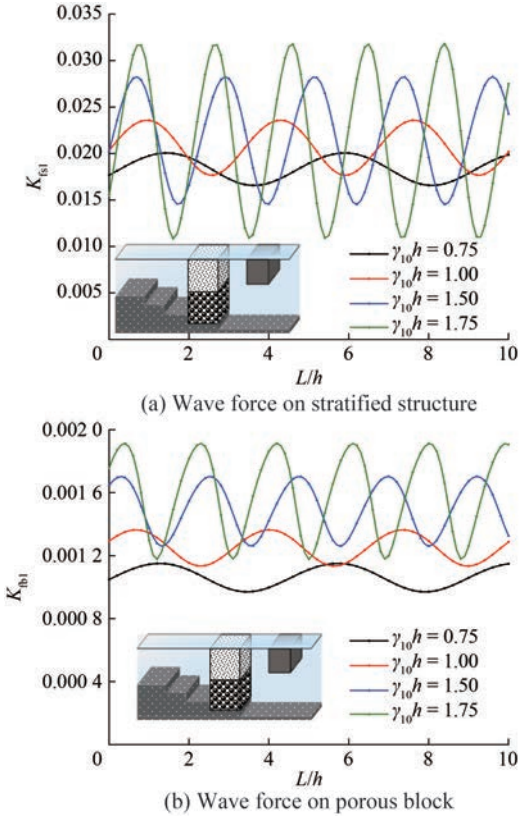

Figure 15 Variation of K_{fs1} and K_{fb1} versus L/h for different values of $\gamma_{10}h$ considering $h_s/h = 0.10$, $a/h = 0.25$, $w_1/h = w_2/h = 0.50$, $\theta = 20°$, $S_2 = S_5 = S_6 = 1$, $\varepsilon_2 = 0.2$, $\varepsilon_5 = 0.7$, $\varepsilon_6 = 0.3$, $f_2 = 0.6$, $f_5 = 0.8$ and $f_6 = 0.5$

The resonating behaviour gradually diminishes as the wavelength increases and tend to attain a more uniform value. For the same L/h value, when $\gamma_{10}h = 1.75$ attains the peak value, K_{fs1} is 86% more compared to that of $\gamma_{10}h = 0.75$. The same trend is observed for K_{fb1} as in Figure 15(b). On varying angle of incidence of wave, the wave force on the front face of the stratified structure and porous block is studied for different dimensionless width of porous block as in Figure 16(a – b). Both K_{fs1} and K_{fb1} is decreasing with increase in angle of incidence. For $w_1/h = 3.0$, K_{fs1} is maximum for $\theta < 10°$ and minimum for $\theta \geqslant 20°$. From Figure 16(a), it is clear that, as the structural width of porous block is increased, wave transmission to the confined region between porous block and stratified structure decreases and hence considerably less wave would be incident on the stratified structure. As a result, wave force acting on the stratified structure would be less. Thus, with the presence of surface-piercing partial structure in combination

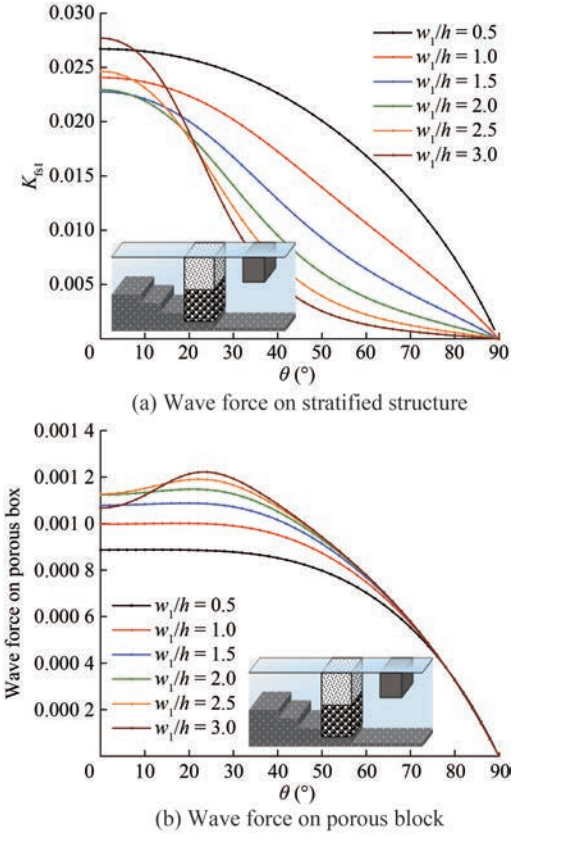

Figure 16 Variation of K_{fs1} and K_{fb1} versus θ for different values of w_1/h considering $\gamma_{10}h = 1.5$, $h_s/h = 0.10$, $a/h = 0.25$, $w_2/h = 0.50$, $L/h = 0.25$, $S_2 = S_5 = S_6 = 1$, $\varepsilon_2 = 0.2$, $\varepsilon_5 = 0.7$, $\varepsilon_6 = 0.4$, $f_2 = 0.6$, $f_5 = 0.8$ and $f_6 = 0.5$

with a fully extended structure, wave force acting on our primary structure can be significantly reduced. As depicted in Figure 16(b), wave force acting on the front face of the porous block increases with increase in width of porous block as most of the incident wave energy is being reflected by the surface-piercing structure.

Further, to study the effect of structural width (Figure 17) on wave transformation, w_1/h is varied from 0.5 to 3.0 against $\gamma_{10}h$. There is considerable variation in K_{fs1} for different w_1/h and it is observed to have peak value at around $\gamma_{10} = 1.5$ for any structural width, as in Figure 15. The wave force on stratified structure is observed to be decreasing for wider surface-piercing porous blocks. Beyond $\gamma_{10}h = 5$, for smaller structural widths, K_{fs1} again increases whereas for larger structural widths, K_{fs1} becomes constant.

4.3 Vertically stratified porous structure with surface-piercing porous block

The wave transformation due to the vertically stratified porous structure combined with porous block in changing bottom topography is analyzed on studying the wave reflection coefficient K_r, transmission coefficient K_t, dissipation

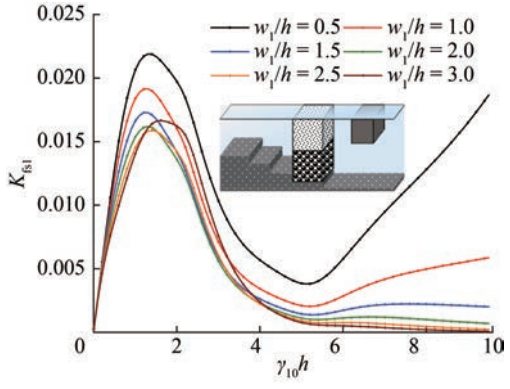

Figure 17 Variation of K_{fs1} versus $\gamma_{10}h$ for different values of w_1/h considering $h_s/h = 0.10$, $a/h = 0.25$, $L/h = 0.25$, $w_2/h = 0.50$, $\theta = 20°$, $S_2 = S_5 = S_6 = 1$, $\varepsilon_2 = 0.2$, $\varepsilon_5 = 0.7$, $\varepsilon_6 = 0.4$, $f_2 = 0.6$, $f_5 = 0.8$ and $f_6 = 0.5$

coefficient K_d, surface displacement $\zeta_j(x)$, wave force acting on the front face of porous block K_{fb1} and on the stratified structure K_{fs1}.

4.3.1 Reflection, transmission and dissipation coefficient

The wave reflection, transmission and dissipation coefficients are analysed for the change in porosity, change in structural width, change in dimensionless wave number and change in the angle of incidence.

4.3.1.1 Effect of multiple porosities

In Figure 18, the vertically stratified porous structure combined with porous block in the presence of stepped bottom topography is analyzed for hydrodynamic coefficients, varying the dimensionless width of porous block and for different combinations of porosities of seaward and leeward porous layers. A mono resonating behaviour is observed for K_r in Figure 18(a) which becomes more prominent as porosity of seaward layer increases. Minimum K_r is observed for the combination of $\varepsilon_5 = 0.9$ and $\varepsilon_6 = 0.1$ when $w_2/h = 0.75$. Thus, this structural width can be used while designing the structure to achieve minimum wave reflection. The reason for zero wave reflection may be that the incoming and reflected waves become 180° out of phase. The K_t value is also considerably reduced as porosity of seaward layer increases and that of leeward porous layer decreases. This can be due to more wave trapping while passing through the porous layers. Compared to horizontally stratified structure in combination with porous block, the combination of vertically stratified structure and porous block showed less K_r and K_t, resulting in more wave energy dissipation as given in Figure 18(b). This may be because, most of the surface concentrated waves are being reflected and dissipated by the surface-piercing porous block and the remaining incident on the stratified structure would be reflected and trapped effectively within the porous layers of vertically stratified structure. The effective trapping is possible when the difference between porosity of seaward and leeward porous layer become larger as observed in the combination of $\varepsilon_5 = 0.9$ and $\varepsilon_6 = 0.1$.

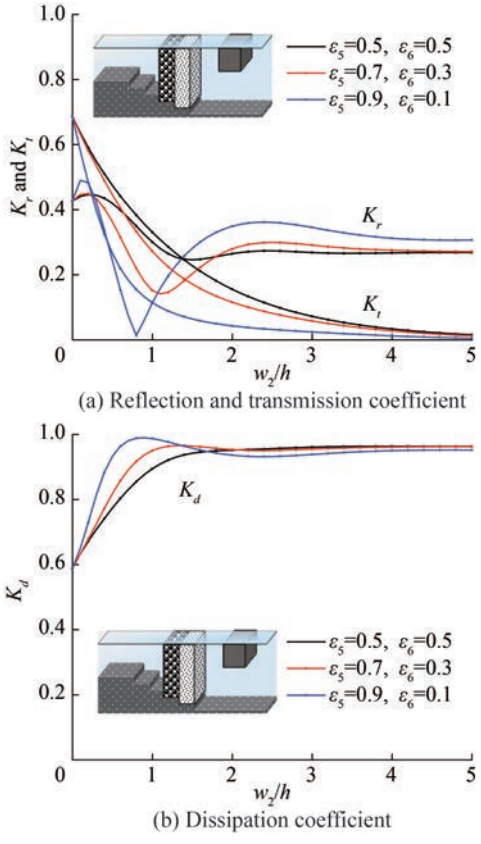

Figure 18 Variation of K_r, K_t and K_d versus w_2/h for different combinations of porosities considering $\gamma_{10}h = 1.5$, $h_s/h = 0.10$, $w_1/h = 0.50$, $L/h = 0.25$, $\theta = 20°$, $S_2 = S_5 = S_6 = 1$, $\varepsilon_2 = 0.2$, $f_2 = 0.6$, $f_5 = 0.8$ and $f_6 = 0.5$

The hydrodynamic characteristics of vertically stratified porous structure combined with porous block is again studied with various combinations of porosity varying dimensionless wavelength. In Figure 19 it is observed that the reflection coefficient is same for all combinations of porosity except that the sudden drop of K_r shows different minimum value for different combinations. This sudden reduction in K_r may be due to the destructive interference. The critical wavelength for which reflection coefficient is minimal is observed to be near to $\lambda/h = 3.0$. The critical wavelength decreases as the porosity of seaward layer is increased and that of leeward layer is decreased. Further, for dimensionless wavelength beyond the critical wavelength, an increase in K_r is observed. In the case of wave transmission coefficient, a considerable decrease in K_t is observed for $\varepsilon_5 = 0.75$ and $\varepsilon_6 = 0.15$. Thus, this combination of porosity may be suitable while designing the vertically stratified structure to achieve less reflection and transmission simultaneously and thereby more wave energy attenuation.

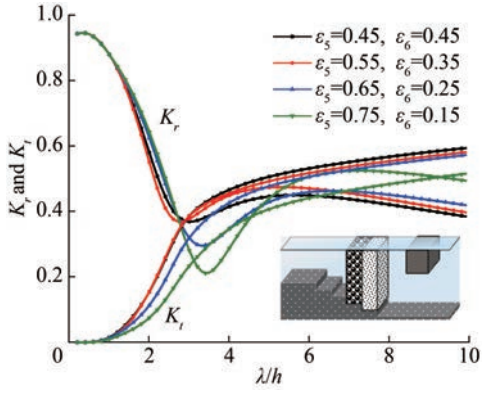

Figure 19 Variation of $K_r$and K_t versus λ/h for different combinations of porosities considering $h_s/h = 0.10$, $a/h = 0.25$, $w_1/h = w_2/h = 0.50$, $L/h = 0.25$, $\theta = 20°$, $S_2 = S_5 = S_6 = 1$, $\varepsilon_2 = 0.2$, $f_2 = 0.6$, $f_5 = 0.8$ and $f_6 = 0.5$

4.3.1.2 Effect of structural width of porous block and stratified structure

To examine the dependence of hydrodynamic properties on structural width of the structure, the wave reflection, transmission, and dissipation coefficients versus λ/h is studied for $0.5 < w_1/h < 2.0$. It can be inferred from Figure 20(a) that due to the presence of the structure, wave reflection coefficient first decreases up to a minimum value and then achieves a nearly stable value for $\lambda/h > 4$. Also, for wider structures, as observed in the case of horizontally stratified structure, reflection coefficient is more while the transmission coefficient is less. However, the decrease in K_r is more prominent than increase in K_t for less wider structures, which helps in improving the wave dissipation characteristics as observed in Figure 20(b). For $\lambda/h = 2$, a decrease in w_1/h from 2.0 to 0.5, increased K_d by four times. A sudden drop in K_d is observed for $w_1/h = 2.0$ due to high wave reflection and less transmission of incoming wave energy.

Further, to understand the significance of width of stratified structure in influencing hydrodynamic behaviour, different values of w_2/h in the range $0.5 \leqslant w_2/h \leqslant 3.0$ are varied against dimensionless wavenumber. It can be inferred from Figure 21(a) that, for shorter waves, K_r is nearly the same irrespective of the width of stratified structure. However, for further increase in λ/h, K_r sharply decreases to a critical value and then increases. The local minima shift towards right with increase in width of stratified structure, may be due to the phase shift when waves encounter more wider structure. In addition, the wave transmission decreases with increase in structural width. For shorter waves, K_t is less but K_d remains same for any structural width. As observed in the case of horizontally stratified structure, longer waves require wider sections for effective wave attenuation. Thus, for these longer waves, wave dissipation of upto 97% can be achieved (Figure 21(b)) by the design of wider structures.

4.3.1.3 Effect of angle of incidence

The impact of angle of incidence in wave transformation by vertically stratified porous structure combined with porous block is studied for $0 < \theta < 90°$ varying porosity of seaward and leeward porous layer. In the case of higher angle of incidence, the K_t seems to be considerably less while K_r steeply increases as observed in Figure 22(a). In comparison to horizontally stratified structure, although wave reflection is nearly same transmission can be considerably reduced by the construction of vertically stratified structure of same structural width in combination with the partial porous structure. Wave damping efficiency for any angle of attack less than 60° has a constant value, beyond which K_d sharply decreases (Figure 22(b)).

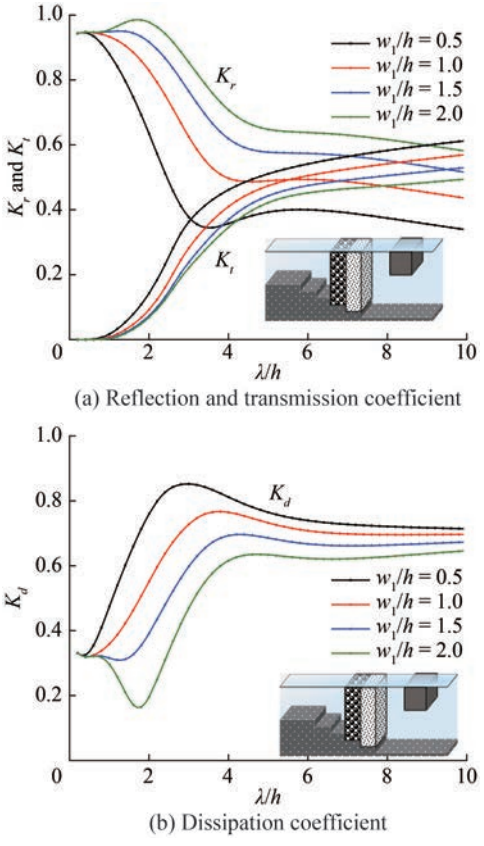

Figure 20 Variation of K_r, K_t and K_d versus λ/h for different values of w_1/h considering $h_s/h = 0.10$, $a/h = 0.25$, $w_2/h = 0.50$, $L/h = 0.25$, $\theta = 20°$, $S_2 = S_5 = S_6 = 1$, $\varepsilon_2 = 0.2$, $\varepsilon_5 = 0.7$, $\varepsilon_6 = 0.3$, $f_2 = 0.6$, $f_5 = 0.8$ and $f_6 = 0.5$

4.3.1.4 Effect of dimensionless wave number

In Figure 23, the hydrodynamic coefficients for the vertically stratified structure combined with porous block in the presence of stepped bottom is analysed for $0.75 < \gamma_{10}h < 1.75$ varying dimensionless width of stratified structure, w_2/h. Slight resonating behaviour is observed for K_r with the minimum value being shifted towards right as the wavenumber decreases due to phase shift and destructive interference. The local maxima correspond to the situation when there is constructive interference between incoming and reflected waves. K_r further increases to achieve a fairly stable value, which increases with decrease in wavelength.

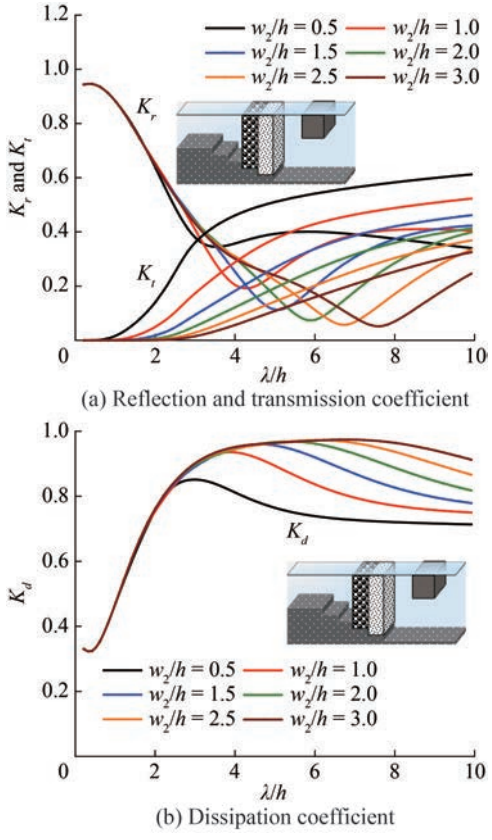

Figure 21 Variation of K_r, K_t and K_d versus λ/h for different values of w_2/h considering $h_s/h = 0.10$, $a/h = 0.25$, $w_1/h = 0.50$, $L/h = 0.25$, $\theta = 20°$, $S_2 = S_5 = S_6 = 1$, $\varepsilon_2 = 0.2$, $\varepsilon_5 = 0.7$, $\varepsilon_6 = 0.4$, $f_2 = 0.6$, $f_5 = 0.8$ and $f_6 = 0.5$

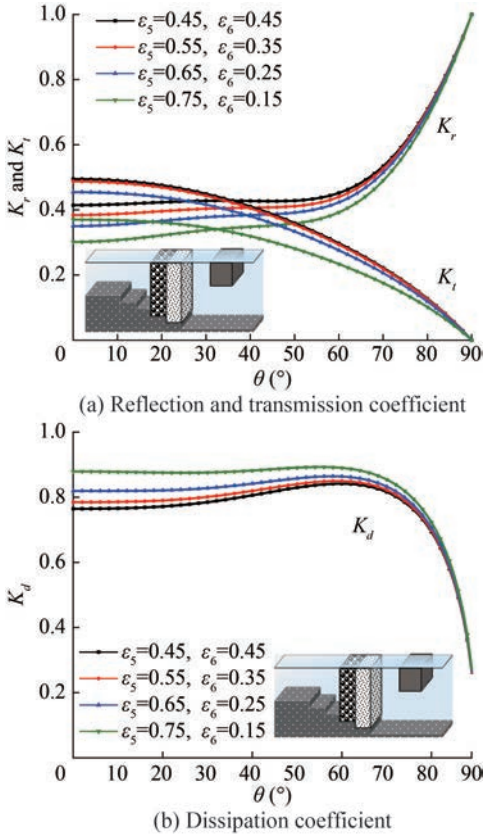

Figure 22 Variation of K_r, K_t and K_d versus θ for different combinations of porosities considering $\gamma_{10}h = 1.5$, $h_s/h = 0.10$, $a/h = 0.25$, $w_1/h = w_2/h = 0.50$, $L/h = 0.25$, $S_2 = S_5 = S_6 = 1$, $\varepsilon_2 = 0.2$, $f_2 = 0.6$, $f_5 = 0.8$ and $f_6 = 0.5$

Wave transmission is on a slightly higher side for longer waves. Compared to the hydrodynamic behaviour of horizontally stratified structure in combination with the porous block, wave reflection and transmission for vertically stratified structure is significantly reduced as observed in previous sections. This is because of effective wave trapping by the vertical layers of stratified structure. For K_d, as shown in Figure 23(b), variation is observed particularly for longer waves only, in the range of $0.5 < \gamma_{10}h < 3$. In contrast to horizontally stratified structure, wave damping was also efficient even for less wider structures.

4.3.2 Surface elevation

In Figure 24, the surface elevation in the incident and transmitted regions for various angle of incidence is observed. The maximum surface elevation is observed in the case of $\theta = 60°$ in the incident open sea region, although there is no considerable variation for different angle of incidence. The reduction in surface elevation by vertically stratified structure is more efficient compared to that of horizontally stratified structure in combination with surface-piercing porous block. There is nearly 60% more decrease in surface elevation for vertically stratified structure. Thus, it is more advisable to construct a vertically stratified porous structure combined with porous block for more tranquil zone in the leeward side.

4.3.3 Wave force on front face of porous block and stratified structure

The wave force on the front face of the stratified structure and porous block is observed to show a resonating behaviour, for varying length between porous block and stratified structure and is plotted for different values of $\gamma_{10}h$ as shown in Figure 25. The wave force due to shorter wave is although more on porous block, it is significantly less when acting on the stratified structure. As observed in Figure 25(b), harmonic crests and troughs tend to be increasing with increase in wavenumber due to more interaction of wave with porous block. Optimum length between porous block and stratified structure so as to have minimum wave force can be determined from the plot while designing the structure. In contrary to the wave force acting on horizontally stratified structure, vertically stratified structure combined with porous block is subjected to less impact of waves. This can be due to less wave reflection and more wave trapping within the structure.

In order to study the wave force on the front face of vertically stratified structure K_{fs1}, different values of

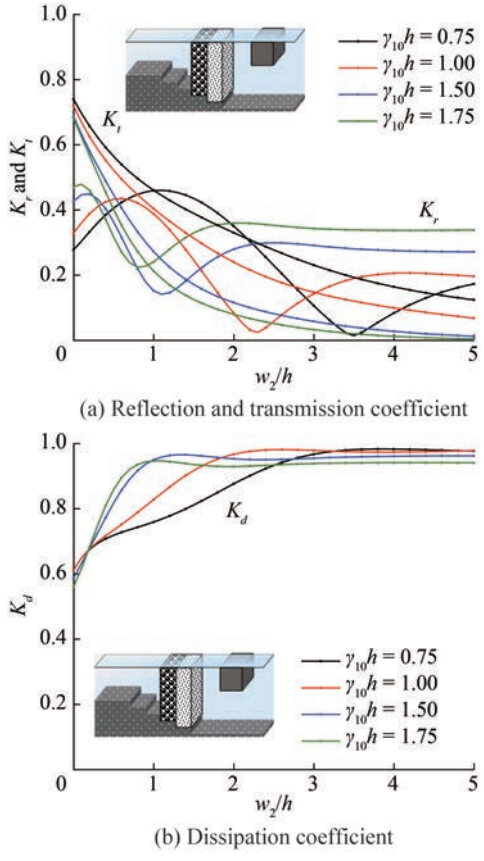

Figure 23 Variation of K_r, K_t and K_d versus w_2/h for different values of $\gamma_{10}h$ considering $h_s/h = 0.10$, $a/h = 0.25$, $w_1/h = 0.50$, $L/h = 0.25$, $\theta = 20°$, $S_2 = S_5 = S_6 = 1$, $\varepsilon_2 = 0.2$, $\varepsilon_5 = 0.7$, $\varepsilon_6 = 0.3$, $f_2 = 0.6$, $f_5 = 0.8$ and $f_6 = 0.5$

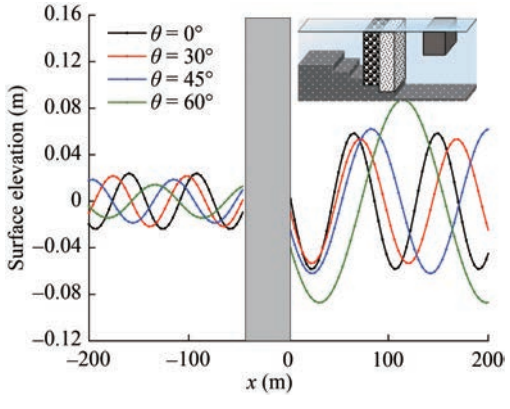

Figure 24 Surface elevation versus x for different values of θ considering $\gamma_{10}h = 1.5$, $h_s/h = 0.10$, $a/h = 0.25$, $w_1/h = w_2/h = 0.50$, $L/h = 0.25$, $S_2 = S_5 = S_6 = 1$, $\varepsilon_2 = 0.2$, $\varepsilon_5 = 0.7$, $\varepsilon_6 = 0.3$, $f_2 = 0.6$, $f_5 = 0.8$ and $f_6 = 0.5$

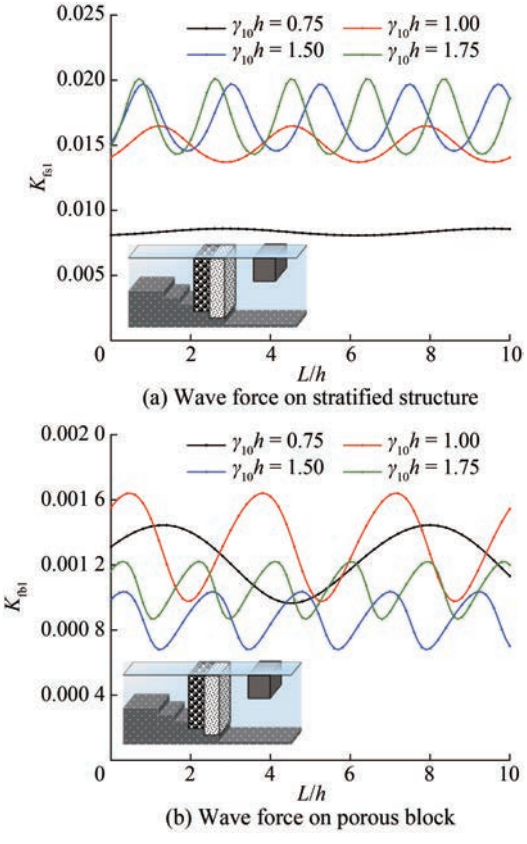

Figure 25 Variation of K_{fs1} and K_{fb1} versus L/h for different values of $\gamma_{10}h$ considering $h_s/h = 0.10$, $a/h = 0.25$, $w_1/h = w_2/h = 0.50$, $\theta = 20°$, $S_2 = S_5 = S_6 = 1$, $\varepsilon_2 = 0.2$, $\varepsilon_5 = 0.7$,$\varepsilon_6 = 0.3$, $f_2 = 0.6$, $f_5 = 0.8$ and $f_6 = 0.5$

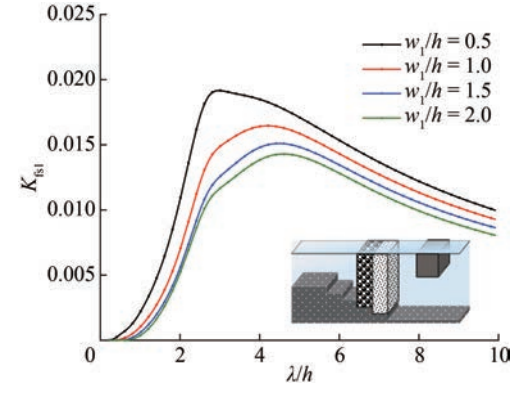

Figure 26 Variation of K_{fs1} versus λ/h for different values of w_1/h considering $h_s/h = 0.10$, $a/h = 0.25$, $w_2/h = 0.50$, $L/h = 0.25$, $\theta = 20°$, $S_2 = S_5 = S_6 = 1$, $\varepsilon_2 = 0.2$, $\varepsilon_5 = 0.7$, $\varepsilon_6 = 0.4$, $f_2 = 0.6$, $f_5 = 0.8$ and $f_6 = 0.5$

w_1/h is considered for varying λ/h. Wave force seems to be increasing with wavelength to attain a peak value and then decreases with further increase in wavelength. This may be due to more reflection that is taking place from the structure for that particular wavelength as a result of constructive interference. Also, it is observed in Figure 26 that wave force decreases with increase in structural width of porous block. This is because, a major part of incident wave energy would be reflected by the wider surface-piercing porous block creating less impact on the stratified structure. However, there are optimum widths of porous block for which wave force can be kept minimal.

In Figure 27(a–b), the wave forces K_{fs1} and K_{fb1} versus w_1/h is analysed for values of $\gamma_{10}h$. The harmonic crests and troughs are observed for both K_{fs1} and K_{fb1} in such a way that harmonic peak is noted increasing with increase in width of porous block. This is more visible in the case of shorter waves due to increased wave interaction with structure and hence more constructive interference takes place between the incident and reflected waves. The values of w_1/h for which wave force is minimum correspond to the optimum width of porous block. As observed in the previous case, K_{fb1} (Figure 27(b)) is considerably more for longer waves.

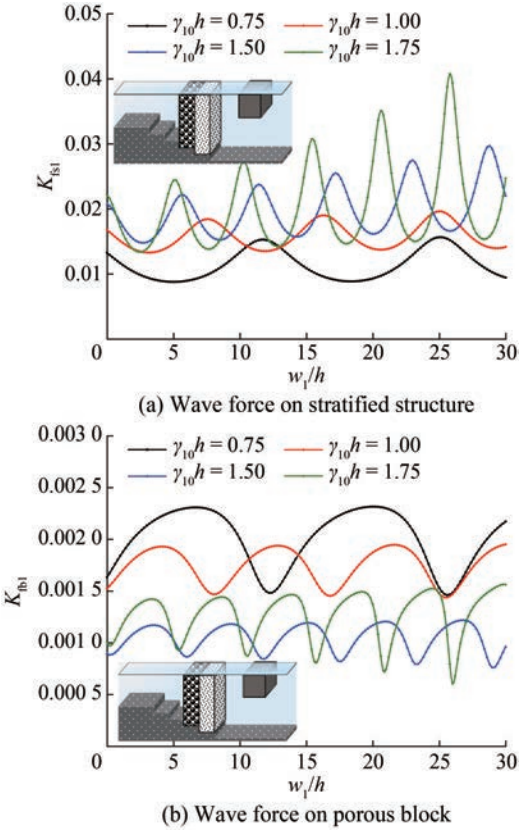

Figure 27 Variation of K_{fs1} and K_{fb1} versus w_1/h for different values of $\gamma_{10}h$ considering $h_s/h = 0.10$, $a/h = 0.25$, $w_2/h = 0.50$, $L/h = 0.25$, $\theta = 20°$, $S_2 = S_5 = S_6 = 1$, $\varepsilon_2 = 0.2$, $\varepsilon_5 = 0.7$, $\varepsilon_6 = 0.4$, $f_2 = 0.6$, $f_5 = 0.8$ and $f_6 = 0.5$

Further to understand the effect of wave force due to varying width of stratified structure, K_{fs1} and K_{fb1} are plotted for varying w_2/h for different values of $\gamma_{10}h$ in Figure 28. For smaller structural width, mono resonating behaviour is observed in K_{fs1} such that shorter waves tend to show peak value at lesser widths of stratified structure due to constructive interference between incoming and reflected waves. The same is observed in the case of K_{fb1}. However, wave forces tend to attain a stable value for wider structures.

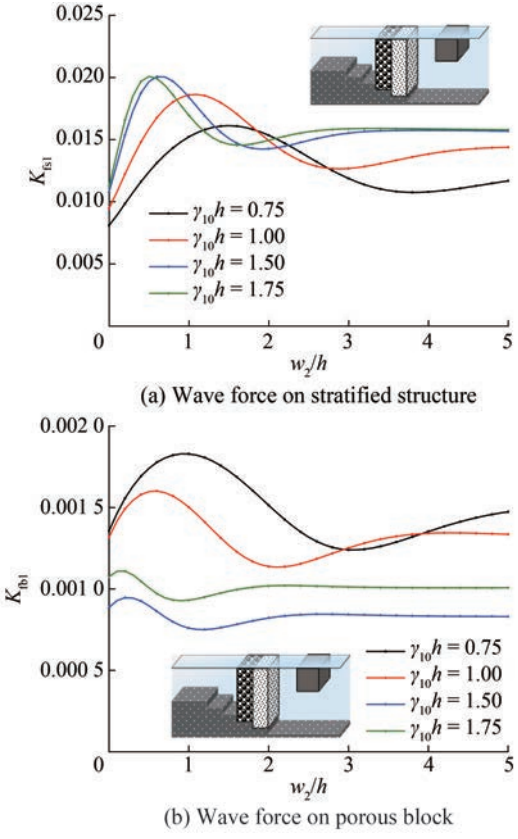

Figure 28 Variation of K_{fs1} and K_{fb1} versus w_2/h for different values of $\gamma_{10}h$ considering $h_s/h = 0.10$, $a/h = 0.25$, $w_1/h = 0.50$, $L/h = 0.25$, $\theta = 20°$, $S_2 = S_5 = S_6 = 1$, $\varepsilon_2 = 0.2$, $\varepsilon_5 = 0.7$, $\varepsilon_6 = 0.3$, $f_2 = 0.6$, $f_5 = 0.8$ and $f_6 = 0.5$

5 Conclusions

The wave transformation due to horizontally and vertically stratified porous structures combined with surface piercing porous block in changing bottom topography is analyzed based on eigenfunction expansion method. The conclusions drawn from the present study are as follows:

• In the case of horizontally stratified structure, least transmission can be achieved for combination of $\varepsilon_5 = 0.7$ and $\varepsilon_6 = 0.3$ along with 20% porosity for surface-piercing block.

• Wave energy dissipation decreases with increase in width of porous block. K_d shows a decrease of 65.28% from $w_1/h = 0.5$ to $w_1/h = 3.0$ in case of horizontally stratified structure combined with porous block.

• In the case of direct angle of incidence, wave transmission decreases by around 82% when width of horizontally stratified porous structure is increased from 0.5 to 3.0 times the water depth.

• Wave reflection for shorter waves is more compared to longer waves. However, wave transmission is least and wave attenuation can be easily achieved due to the presence of the porous block. For longer waves, wave dissipation of

upto 97% can be achieved by designing wider structures.

• The wave force acting on stratified structure can be decreased if the structure is combined with wider surface-piercing porous blocks.

• In the case of vertically stratified porous structure, minimum wave reflection can be achieved for the combination of $\varepsilon_5 = 0.9$ and $\varepsilon_6 = 0.1$ when width of the stratified structure is 0.75 times the water depth.

• The presence of stratified porous structure combined with porous block decreases surface elevation to a large extent.

• Vertically stratified structure combined with the surface-piercing porous block seems to be more efficient in terms of less wave reflection and transmission and thereby high wave energy dissipation compared to vertically stratified structure.

Nomenclature

C_m	Added mass coefficient
C_f	Turbulent resistant coefficient
ε_2	Porosity of the surface piercing porous block
ε_5	Porosity of the surface or seaward porous layer
ε_6	Porosity of the bottom or leeward porous layer
f_2	Frictional coefficient of surface piercing porous block
f_5	Frictional coefficient of surface or seaward porous layer
f_6	Frictional coefficient of bottom or leeward porous layer
g	Acceleration due to gravity
I_{10}	Complex amplitude of incident wave energy
i	Imaginary number
K_d	Energy dissipation coefficient
K_{fb1}	Wave force coefficient on front face of porous block
K_{fs1}	Wave force coefficient on front face of stratified porous structure
k_{jn}	Wave number in x−direction
K_r	Reflection coefficient
K_t	Transmission coefficient
L	Gap between the porous block and stratified porous structure
l	Wave number in z−direction
M	Number of evanescent wave modes
q	Instantaneous Eularian velocity vector
R_{10}	Complex amplitude of reflected wave energy
S_2	Reactance coefficient of surface piercing porous block
S_5	Reactance coefficient of surface or seaward porous layer
S_6	Reactance coefficient of bottom or leeward porous layer
t	Time
T	Wave period
T_{90}	Complex amplitude of transmitted wave energy
V	Volume
w_1	Width of the porous block
w_2	Width of the stratified porous structure
ω	Wave frequency
x	Horizontal distance along x−direction
y	Vertical distance along y−direction
γ_{jn}	Wave number in y−direction
θ	Incident wave angle

Acknowledgement The authors acknowledge Science and Engineering Research Board (SERB), Department of Science & Technology (DST), Government of India for supporting financially under the research grant No. CRG/2018/004184 and Ministry of Ports, Shipping and Waterways, Government of India through the research grant No. DW/01013(13)/2/2021.

Competing interest D. Karmakar is an editorial board member for the Journal of Marine Science and Application and was not involved in the editorial review, or the decision to publish this article. All authors declare that there are no other competing interests.

References

Ashok R, Manam SR (2022) Oblique wave scattering problems involving vertical porous membranes. Journal of Marine Science and Application 21: 51-66. https://doi.org/10.1007/s11804-022-00255-0

Behera H, Ghosh S (2019) Oblique wave trapping by a surface-piercing flexible porous barrier in the presence of step-type bottoms. Journal of Marine Science and Application 18: 433-443. https://doi.org/10.1007/s11804-018-0036-2

Dalrymple RA, Losada MA, Martin PA (1991) Reflection and transmission from porous structures under oblique wave attack. Journal of Fluid Mechanics 224: 625-644. https://doi.org/10.1017/S0022112091001908

Dattatri J, Raman H, Shankar NJ (1978) Performance characteristics of submerged breakwaters. In Coastal Engineering Proceedings, Hamburg, 2153-2171. https://doi.org/10.9753/icce.v16.130

Das S, Bora SN (2014) Reflection of oblique ocean water waves by a vertical rectangular porous structure placed on an elevated horizontal bottom. Ocean Engineering 82: 135-143. https://doi.org/10.1016/j.oceaneng.2014.02.035

Hu J, Zhao Y, Liu PLF (2019) A model for obliquely incident wave interacting with a multi-layered object. Applied Ocean Research 87: 211-222. https://doi.org/10.1016/j.apor.2019.03.004

Karmakar D, Guedes Soares C (2014) Wave transformation due to multiple bottom-standing porous barriers. Ocean Engineering 80: 50-63. https://doi.org/10.1016/j.oceaneng.2014.01.012

Koley S, Behera H, Sahoo T (2015) Oblique wave trapping by porous structures near a wall. Journal of Engineering Mechanics 141(3): 04014122. https://doi.org/10.1061/(ASCE)EM.1943-7889.0000843

Koley S, Sahoo T (2017) Oblique wave trapping by vertical permeable membrane barriers located near a wall. Journal of Marine Science and Application 16: 490-501. https://doi.org/10.1007/s11804-017-1432-8

Kondo H, Toma S (1972) Reflection and transmission for a porous structure. Coastal Engineering Proceedings 1(13): 1847-1866. https://doi.org/10.9753/icce.v13.100

Liu Y, Li H (2013) Wave reflection and transmission by porous breakwaters: A new analytical solution. Coastal Engineering 78:

46-52. https://doi.org/10.1016/j.coastaleng.2013.04.003
Liu Y, Li Y, Teng B (2007) Wave interaction with a new type perforated breakwater. Acta Mech Sin 23(4): 351-358. https://doi.org/10.1007/s10409-007-0086-1
Madsen PA (1983) Wave reflection from a vertical permeable wave absorber. Coastal Engineering 7(4): 381-396. https://doi.org/10.1016/0378-3839(83)90005-4
Mallayachari V, Sundar V (1994) Reflection characteristics of permeable seawalls. Coastal Engineering 23(1-2): 135-150. https://doi.org/10.1016/0378-3839(94)90019-1
Mendez FJ, Losada IJ (2004) A perturbation method to solve dispersion equations for water waves over dissipative media. Coastal Engineering 51(1): 81-89. https://doi.org/10.1016/j.coastaleng.2003.12.007
Sahoo T, Lee MM, Chwang AT (2000) Trapping and generation of waves by vertical porous structures. Journal of Engineering Mechanics 126: 1074-1082. https://doi.org/10.1061/(ASCE)0733-9399(2000)126:10(1074)
Sollitt CK, Cross RH (1972) Wave transmission through permeable breakwaters. In Coastal Engineering, 1827-1846. https://doi.org/10.9753/icce.v13.99
Somervell LT, Thampi SG, Shashikala AP (2017) A novel approach for the optimal design of a vertical cellular breakwater based on multi-objective optimization. Coastal Engineering Journal 59(4): 1750019. https://doi.org/10.1142/S057856341750019X
Sulisz W (1985) Wave reflection and transmission at permeable breakwaters of arbitrary cross-section. Coastal Engineering 9(4): 371-386. https://doi.org/10.1016/0378-3839(85)90018-3
Tabssum S, Kaligatla RB, Sahoo T (2020) Gravity wave interaction with a porous breakwater in a two-layer ocean of varying depth. Ocean Engineering 196: 106816. https://doi.org/10.1016/j.oceaneng.2019.106816
Twu SW, Chieu CC (2000) A highly wave dissipation offshore breakwater. Ocean Engineering 27(3): 315-330. https://doi.org/10.1016/S0029-8018(99)00002-5
Twu SW, Lin DT (1990) Wave reflection by a number of thin porous plates fixed in a semi-infinitely long flume. In Coastal Engineering Proceedings, Delft, 1046-1059. https://doi.org/10.1061/9780872627765.081
Twu SW, Liu CC, Twu CW (2002) Wave damping characteristics of vertically stratified porous structures under oblique wave action. Ocean Engineering 29(11): 1295-1311. https://doi.org/10.1016/S0029-8018(01)00091-9
Venkateswarlu V, Praveen KM, Karmakar D (2020a) Surface gravity wave scattering by multiple energy absorbing structures of variable horizontal porosity. Coastal Engineering Journal 62(4): 504-526. https://doi.org/10.1080/21664250.2020.1794274
Venkateswarlu V, Karmakar D (2020b) Significance of seabed characteristics on wave transformation in the presence of stratified porous block. Coastal Engineering Journal 62(1): 1-22. https://doi.org/10.1080/21664250.2019.1676366
Venkateswarlu V, Karmakar D (2020c) Wave motion over stratified porous absorber combined with seaward vertical barrier. Proceedings of the Institution of Mechanical Engineers, Part M: Journal of Engineering for the Maritime Environment 234(4): 830-845. https://doi.org/10.1177/1475090220912643
Yu X, Chwang AT (1994) Wave motion through porous structures. Journal of Engineering Mechanics 120(5): 989-1008. https://doi.org/10.1061/(ASCE)0733-9399(1994)120:5(989)
Zhu S, Chwang AT (2001) Analytical study of porous wave absorber. Journal of Engineering Mechanics 127(4): 326-332. https://doi.org/10.1061/(ASCE)0733-9399(2001)127:4(326)